ELECTRON AND PROTON SCATTERING ON STABLE AND EXOTIC NUCLEI

Carlotta Giusti
Università and INFN, Pavia

ECT* Workshop: Probing exotic structure of short-lived nuclei by electron scattering - ECT* Trento 16-20 July 2018

WHY ELECTRON SCATTERING ?

- powerful tool to investigate nuclear structure and dynamics
- predominantly EM interaction, QED, weak compared with nuclear int.
- BA one-photon exchange approx

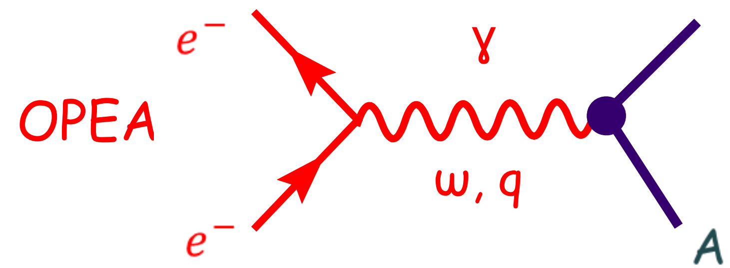

- photon can explore the whole target volume
- independently vary (ω, q) : it is possible to map the nuclear response as a function of its excitation energy with a spatial resolution that can be adjusted to the scale of the processes that need to be studied

NUCLEAR RESPONSE

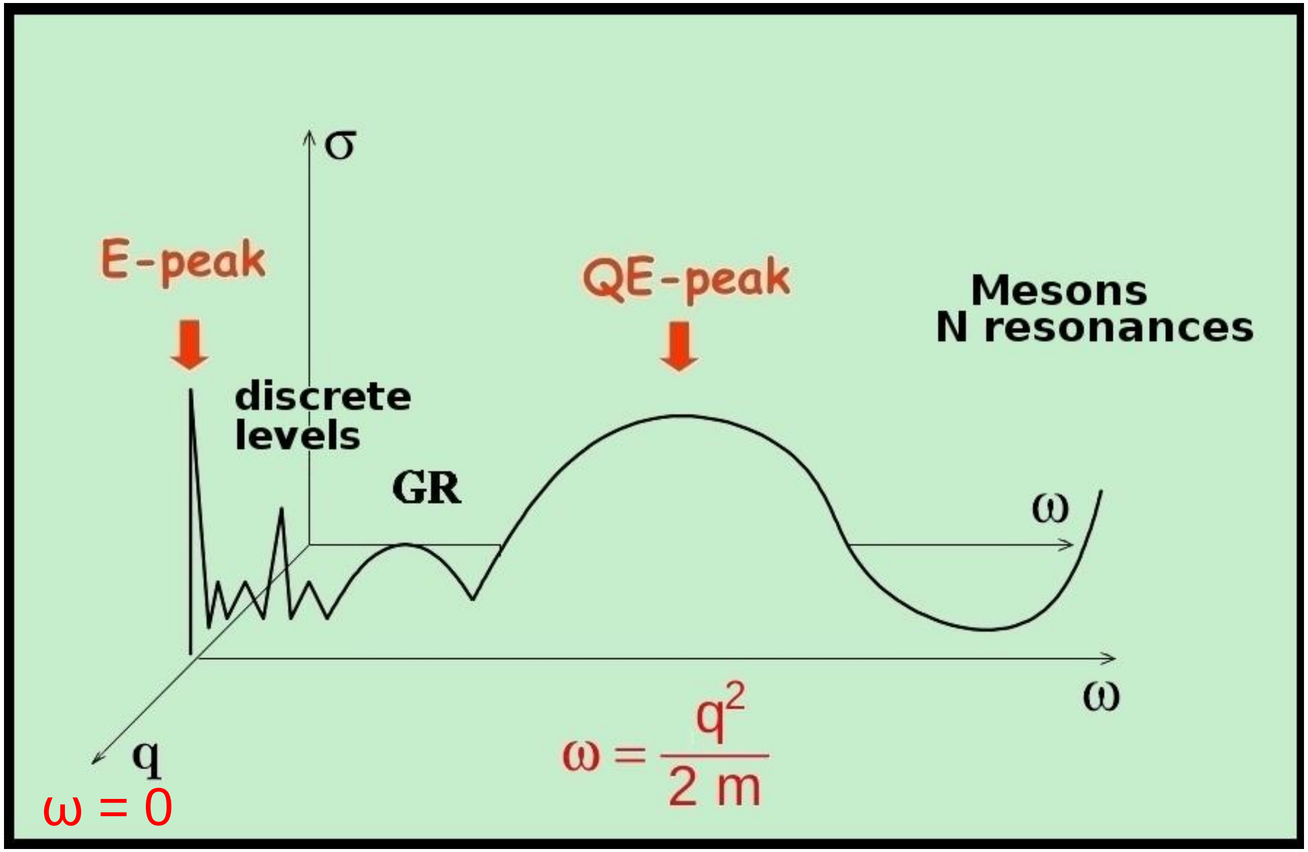

NUCLEAR RESPONSE

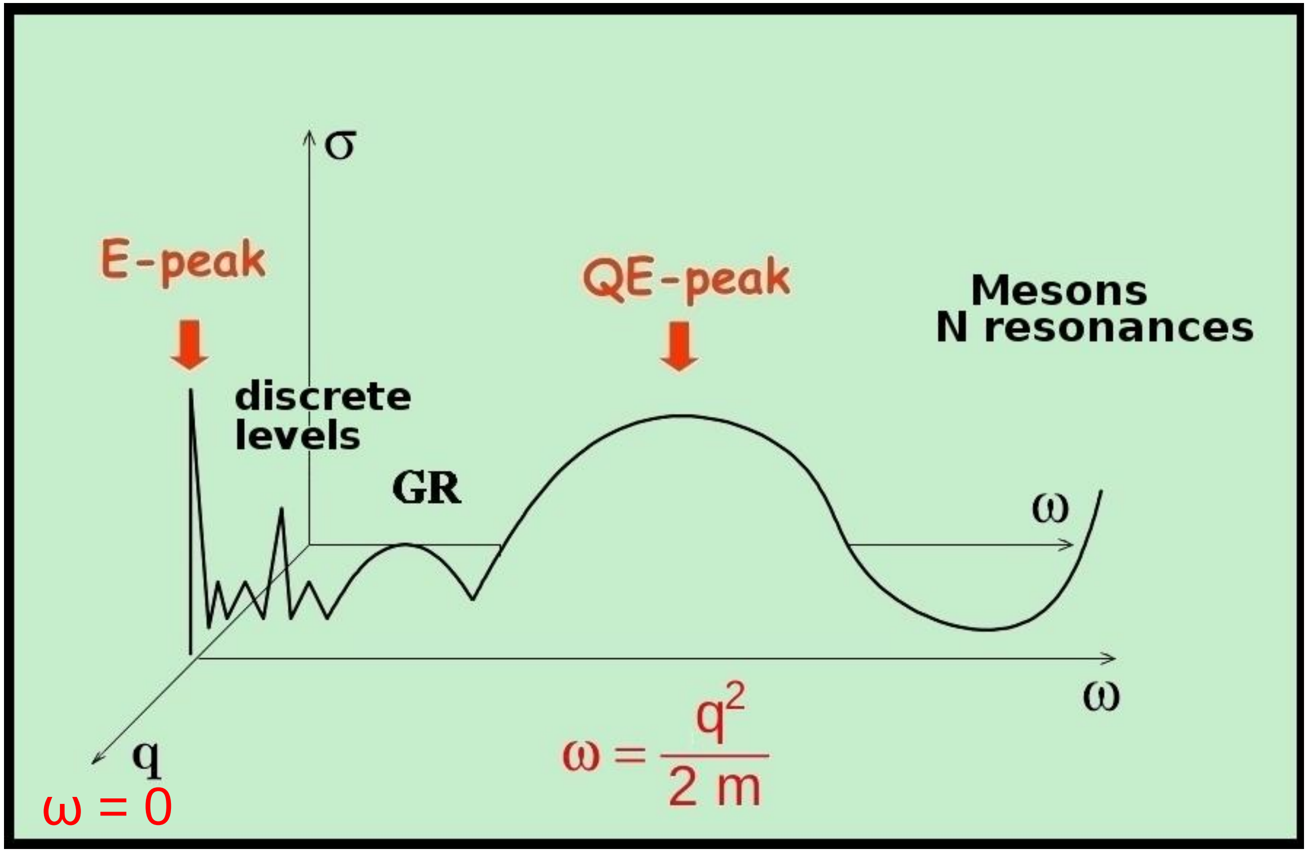

g.s. properties
charge densities, current distr.
charge radii

NUCLEAR RESPONSE

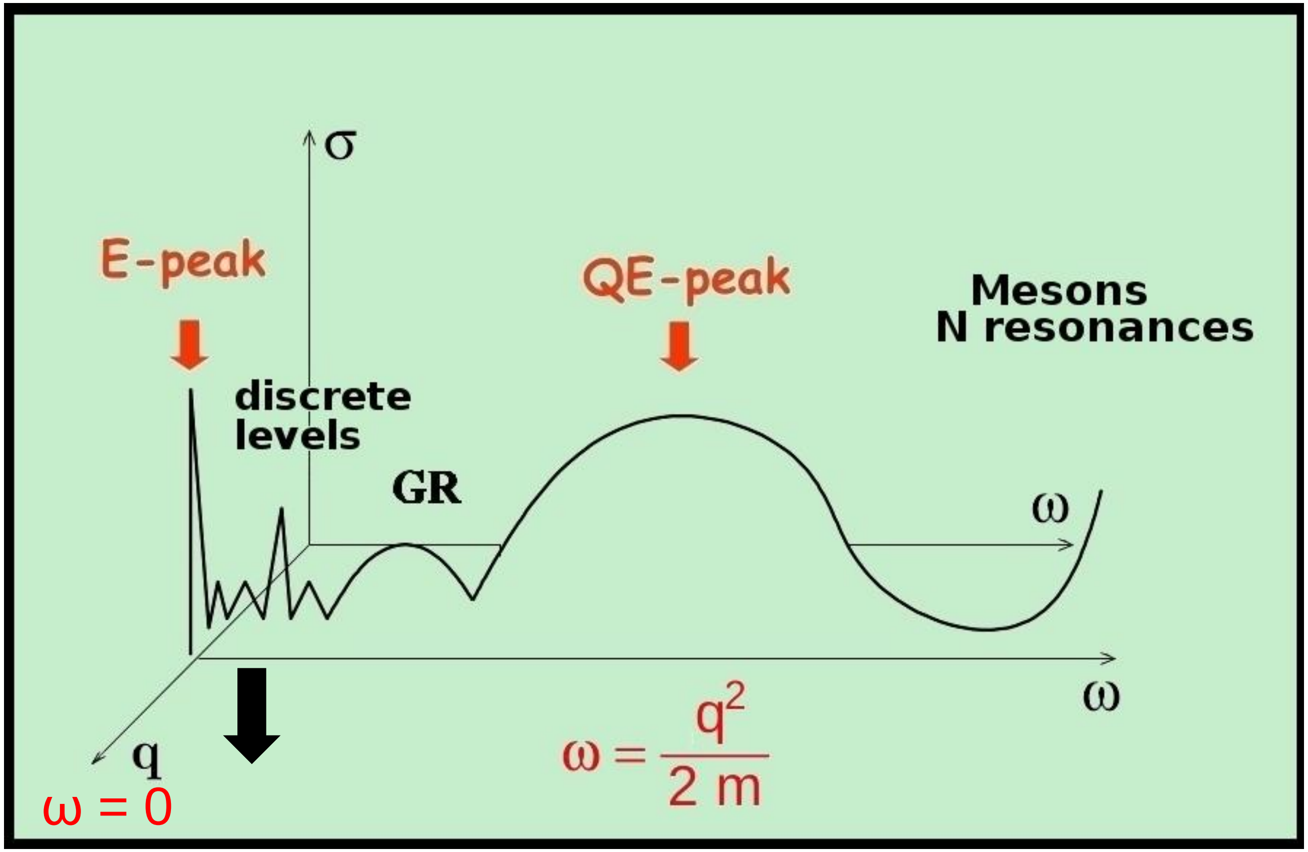

inelastic scattering
discrete excited states

NUCLEAR RESPONSE

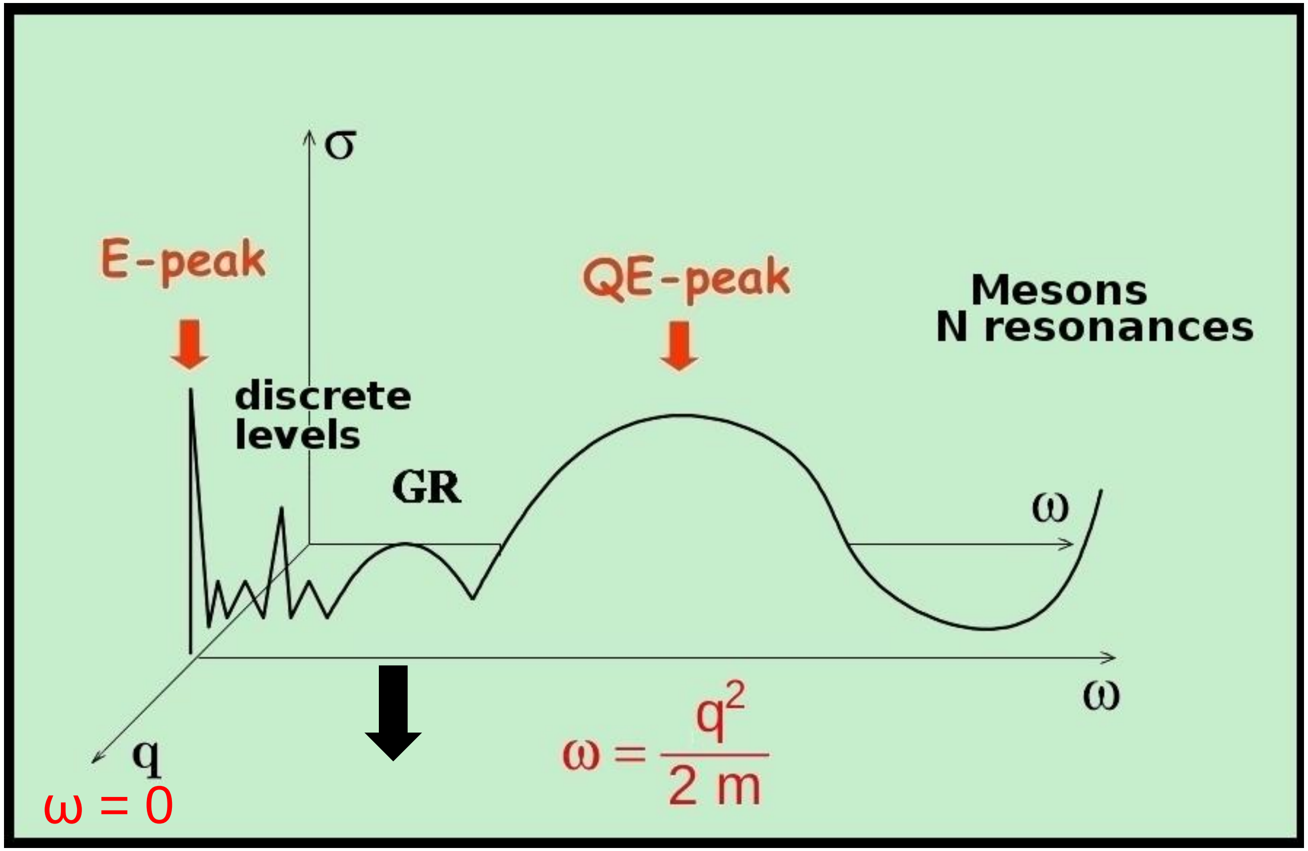

beyond particle emission threshold:
GR collective excitations
electric and magnetic giant multipole resonances

NUCLEAR RESPONSE

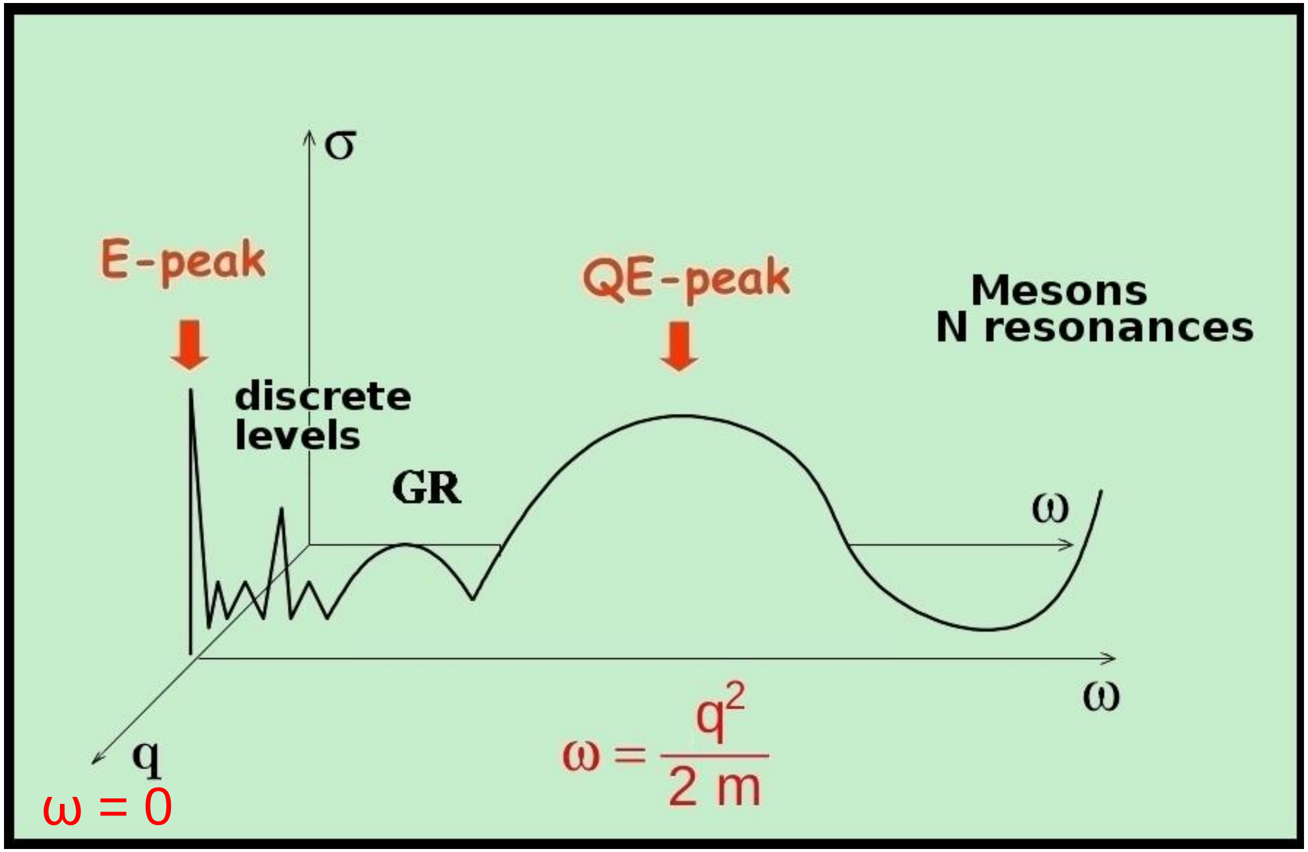

quasi-free process
one-nucleon knockout
s.p. properties, energy and mom. distr.

NUCLEAR RESPONSE

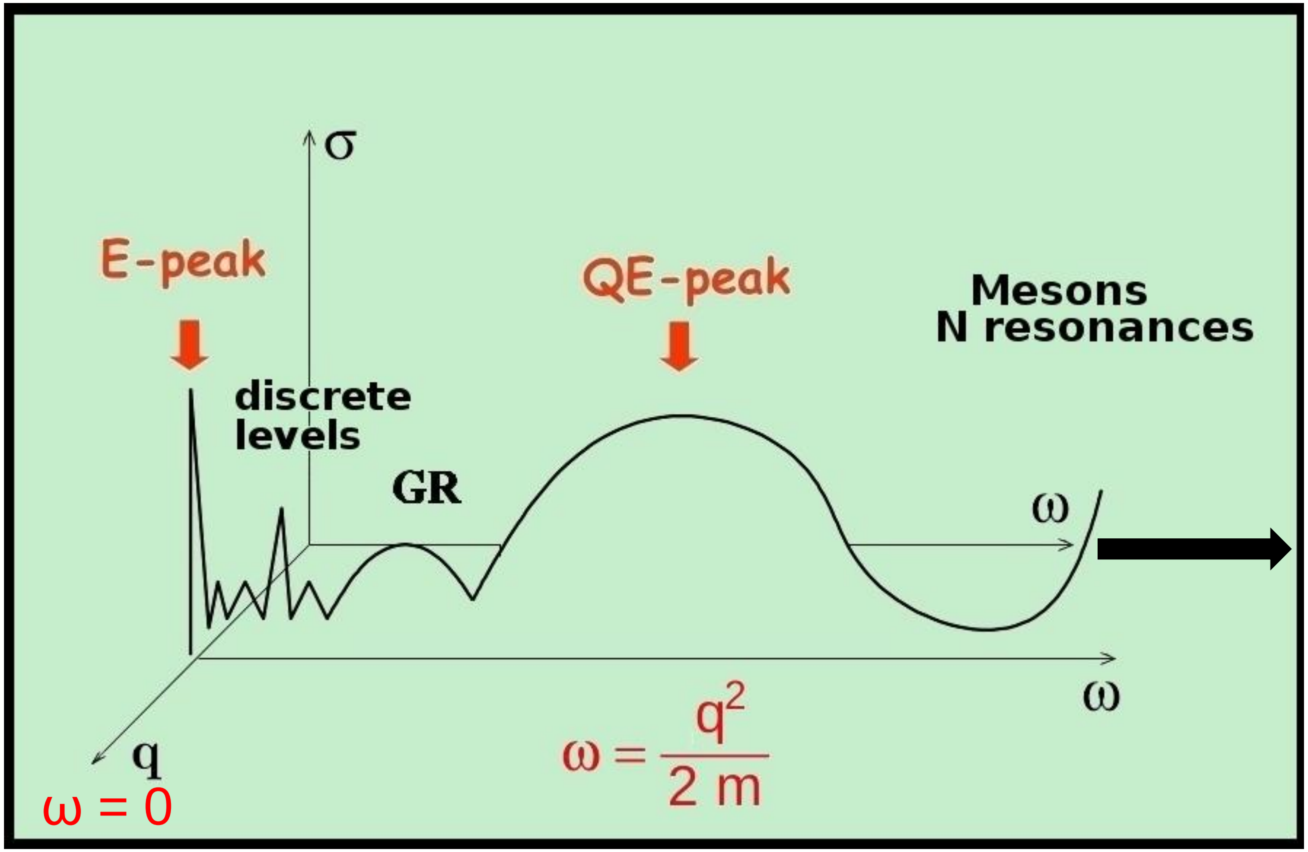

Δ, N^*, nucleon resonances, mesons, deep inelastic scattering…….

NUCLEAR RESPONSE

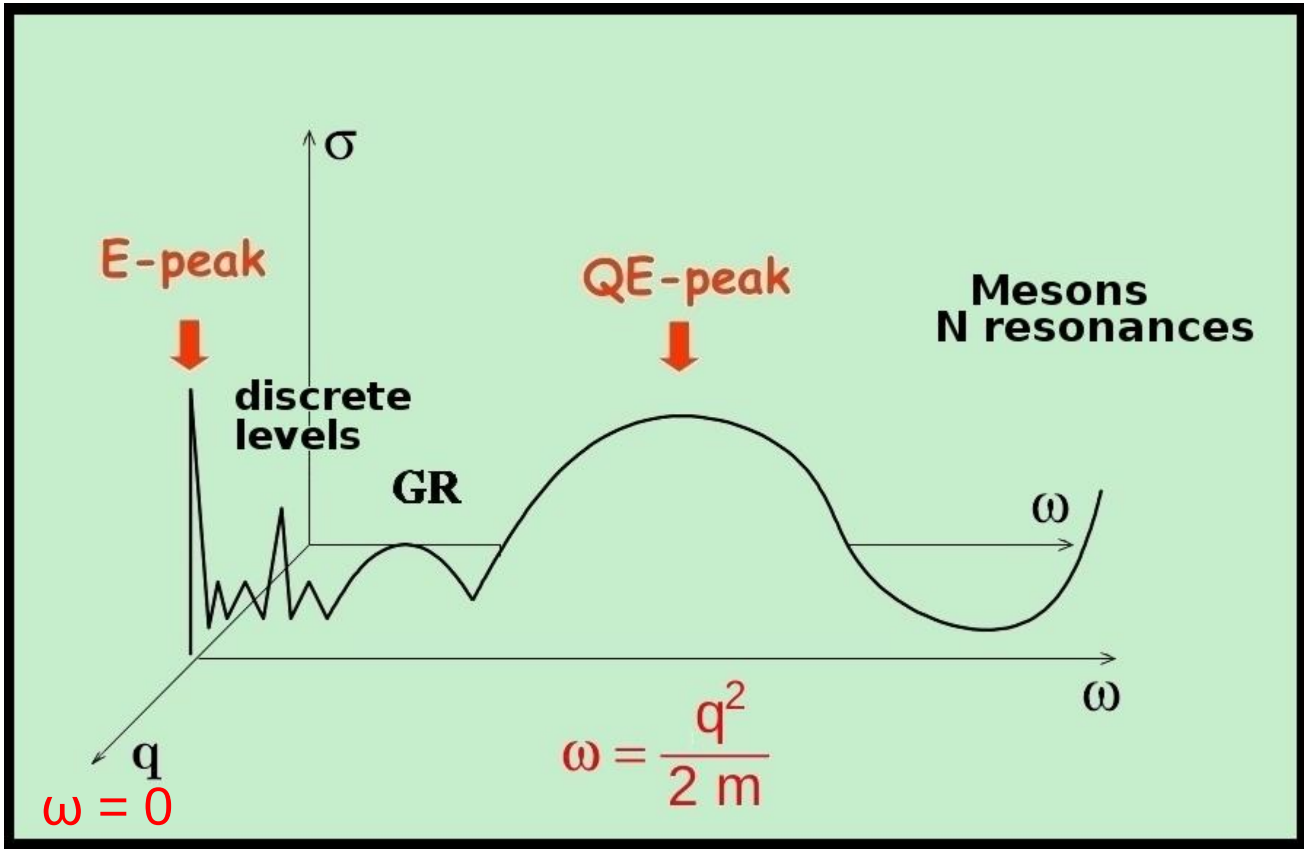

global g.s. properties

s.p properties

ELECTRON AND PROTON SCATTERING ON STABLE AND EXOTIC NUCLEI

- E and QE eA scattering:
- detailed information obtained for stable nuclei
- electron scattering can be extended to unstable nuclei
- understanding the evolution of nuclear properties as a function of N/Z asymmetry
- models tested in comparison with available data applied to isotopic chains
- evolution of nuclear properties with models of proven reliability in stable isotopes will test the ability of the established nuclear theory in the domain of exotic nuclei
- elastic eA (p distrib.) pA scattering (p and n distribution)
- optical potential for elastic pA and QE eA scattering

ELASTIC ELECTRON-NUCLEUS SCATTERING

PWBA

V_{coul} neglected, PW for electrons

$$\frac{d\sigma}{d\omega} = \sigma_M \; | F_p \, (q) \, |^2$$

Mott c.s.

charge form factor
charge density distr.

DWBA

V_{coul} DW for electrons: solve partial wave Dirac eq.
c.s. still reflects the behavior of the charge proton density distribution

NUCLEAR DENSITY DISTRIBUTION

- RMF using a DDME where the couplings between meson and baryon fields are functions of the density

- RMF: nucleus system of Dirac nucleons coupled to the exchange mesons (σ, ω, ρ) and elm field through an effective Lagrangian, whose parameters adjusted to reproduce NM EOS and global properties of spherical closed-shell nuclei

- Open-shell nuclei require unified and self-consistent treatment of MF and pairing correlations: RHB

neutron and proton density distributions

Ca isotopes

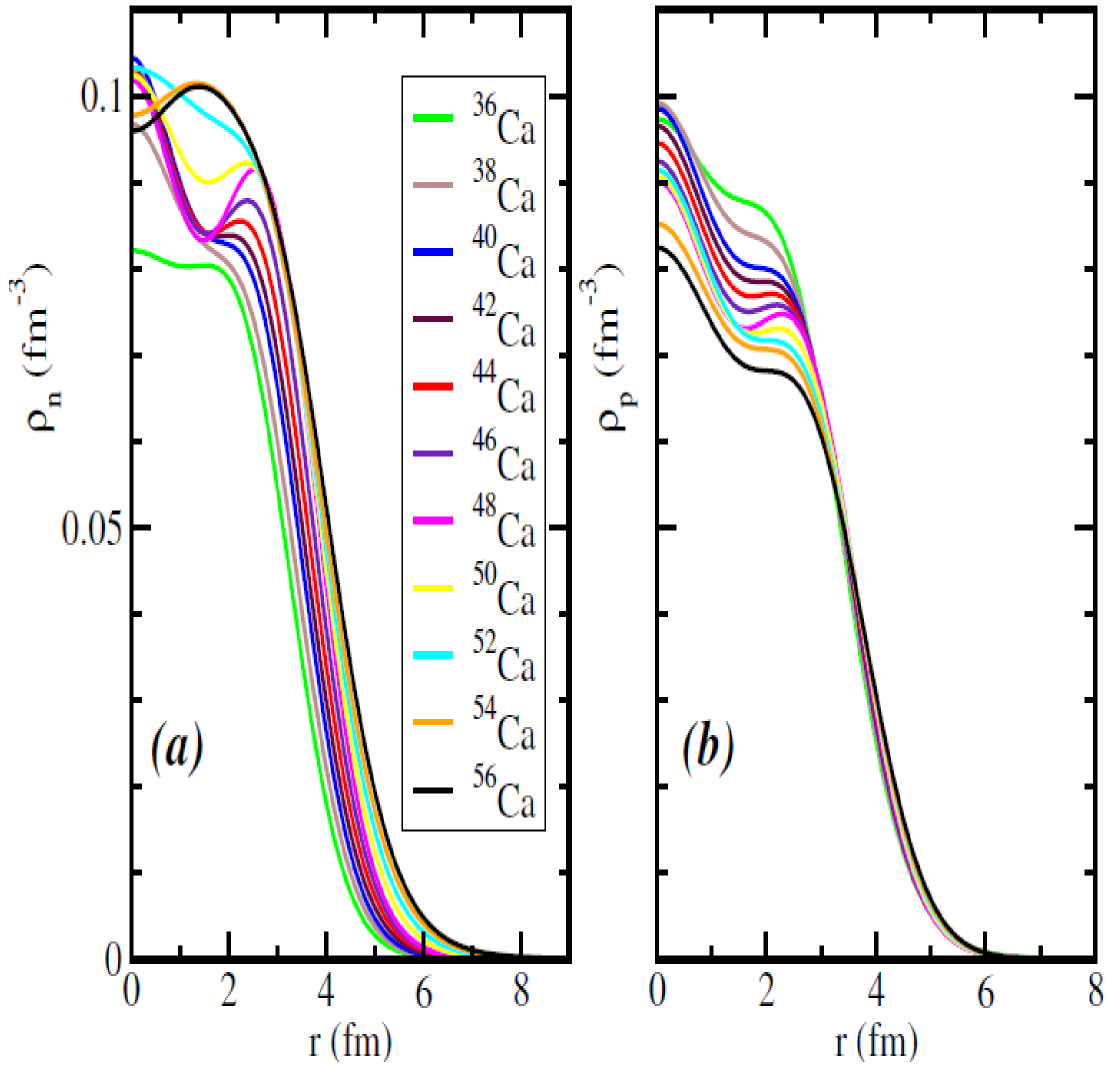

A. Meucci, M. Voraabi, C. Giusti, F.D. Pacati, P. Finelli, PRC 87 054620 (2013)

neutron and proton density distributions

Ca isotopes

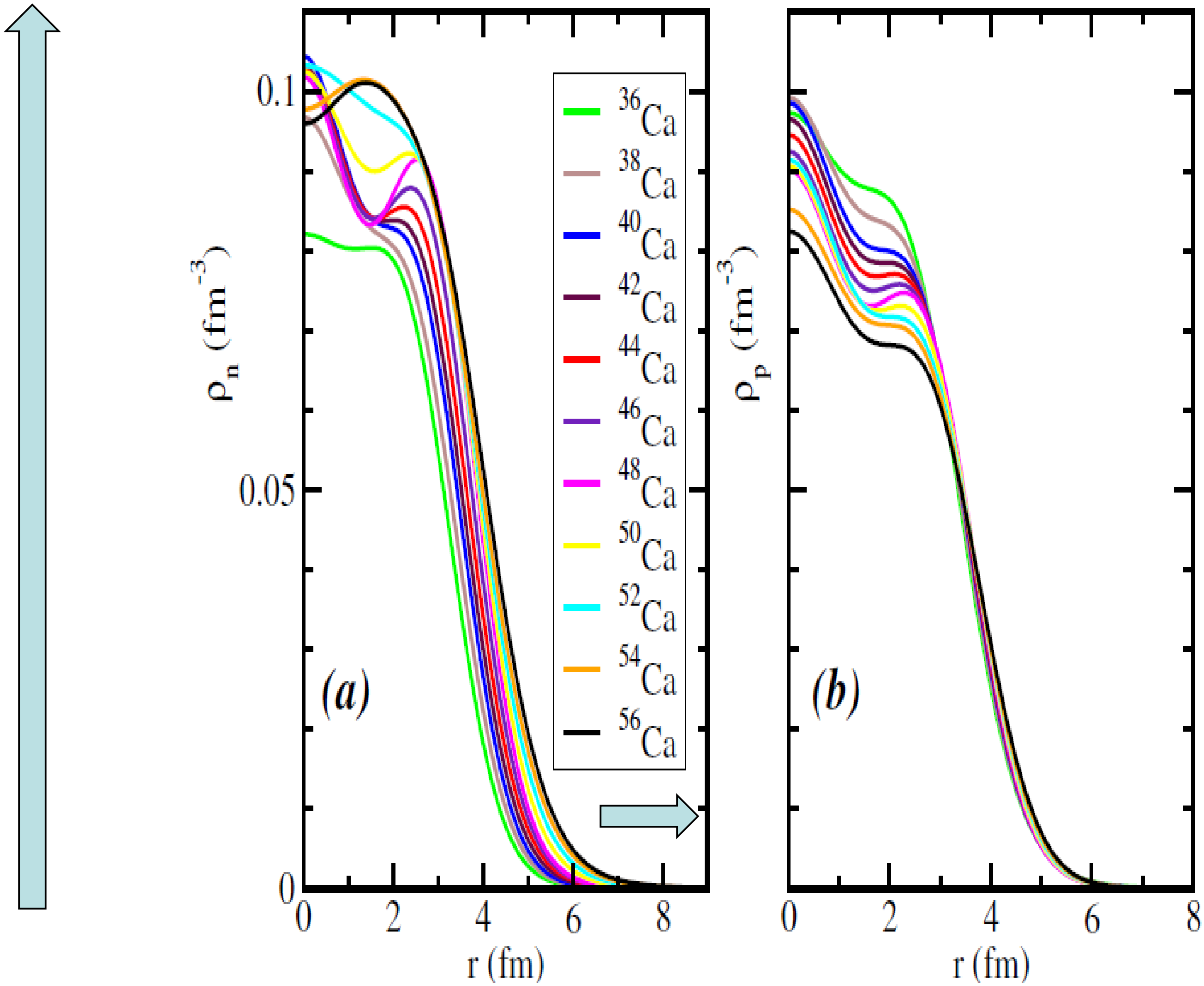

A. Meucci, M. Voraabi, C. Giusti, F.D. Pacati, P. Finelli, PRC 87 054620 (2013)

neutron and proton density distributions

Ca isotopes

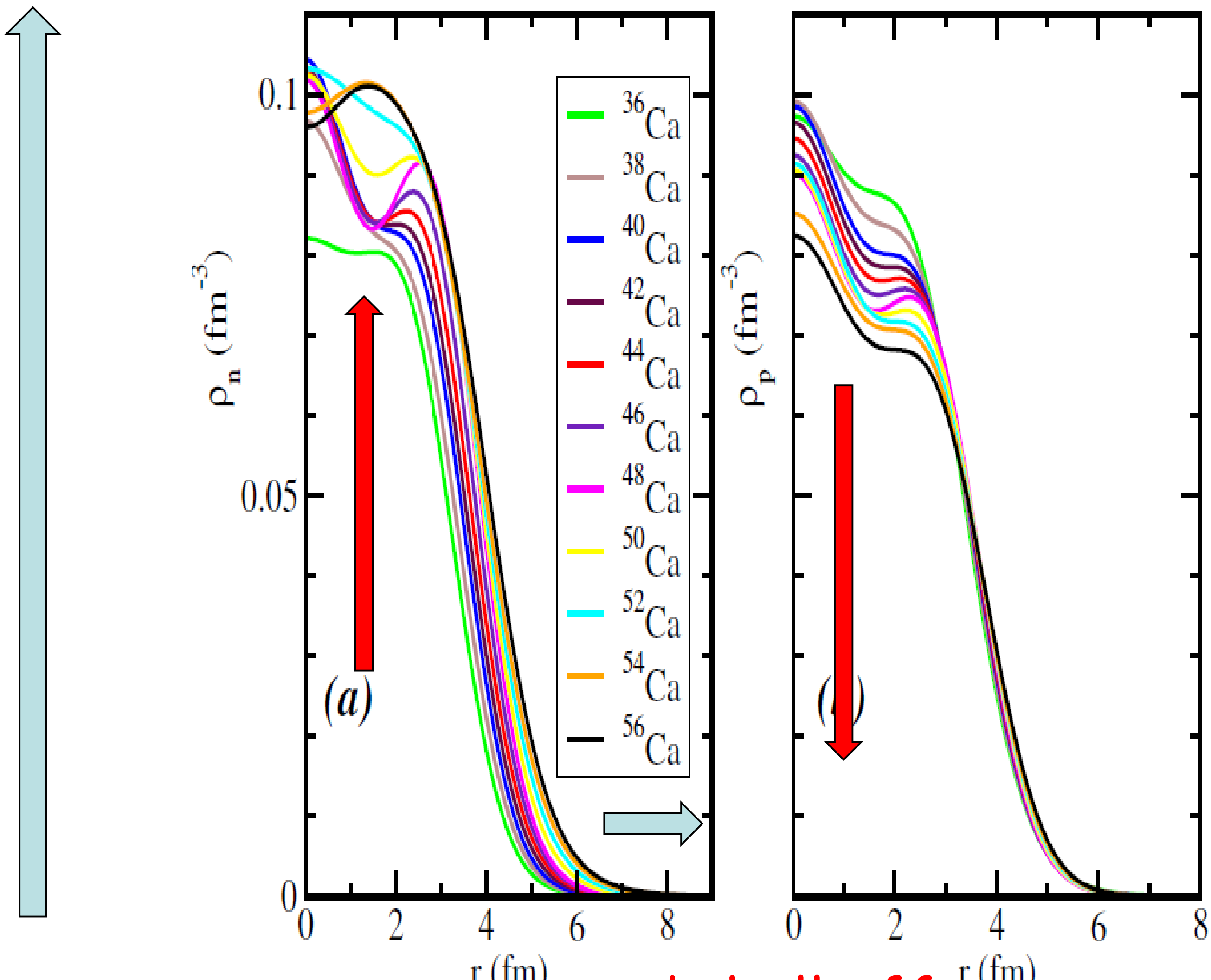

pronounced shell effects

A. Meucci, M. Voraabi, C. Giusti, F.D. Pacati, P. Finelli, PRC 87 054620 (2013)

ELASTIC ELECTRON SCATTERING: DWBA

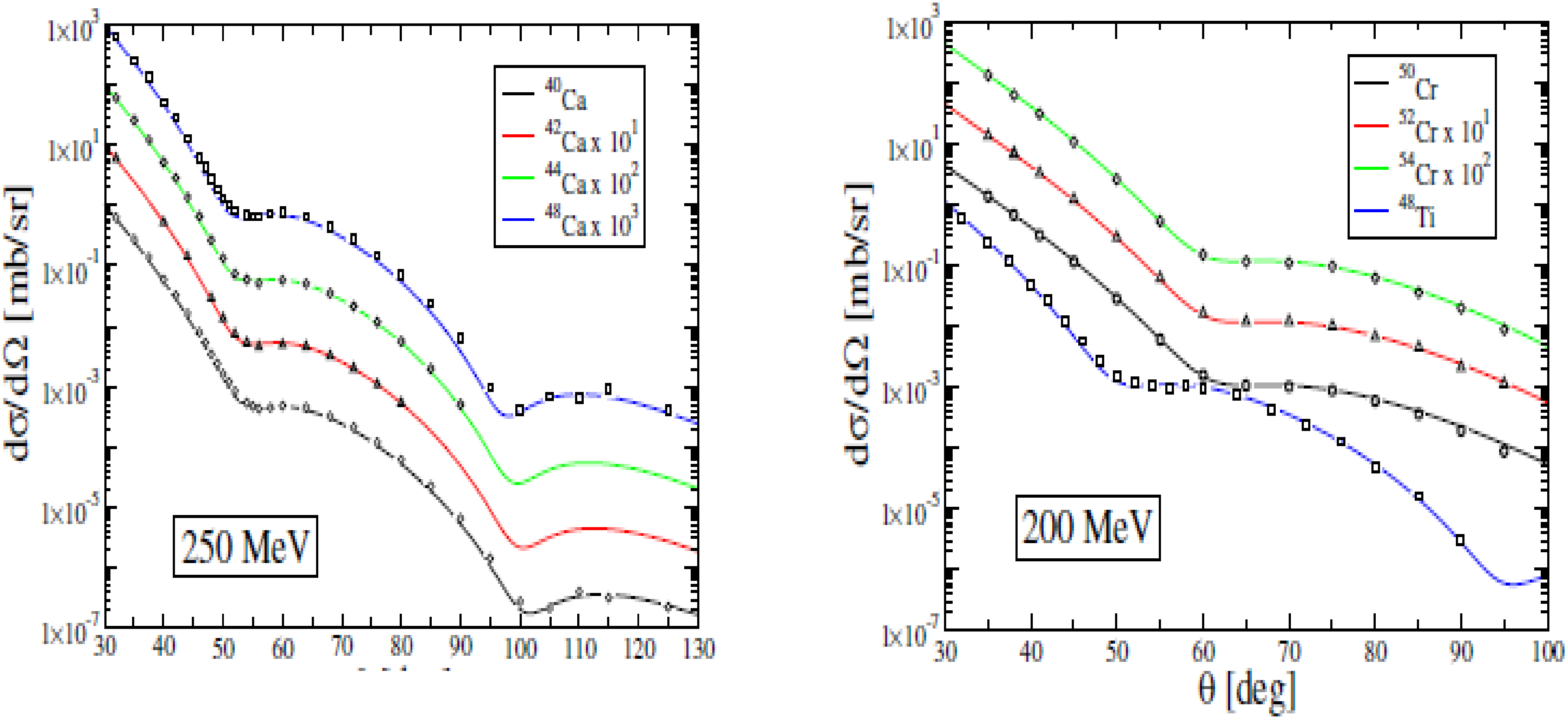

A. Meucci, M. Voraabi, C. Giusti, F.D. Pacati, P. Finelli, PRC 89 034604 (2014)

ELASTIC ELECTRON SCATTERING: DWBA

Ca isotopes

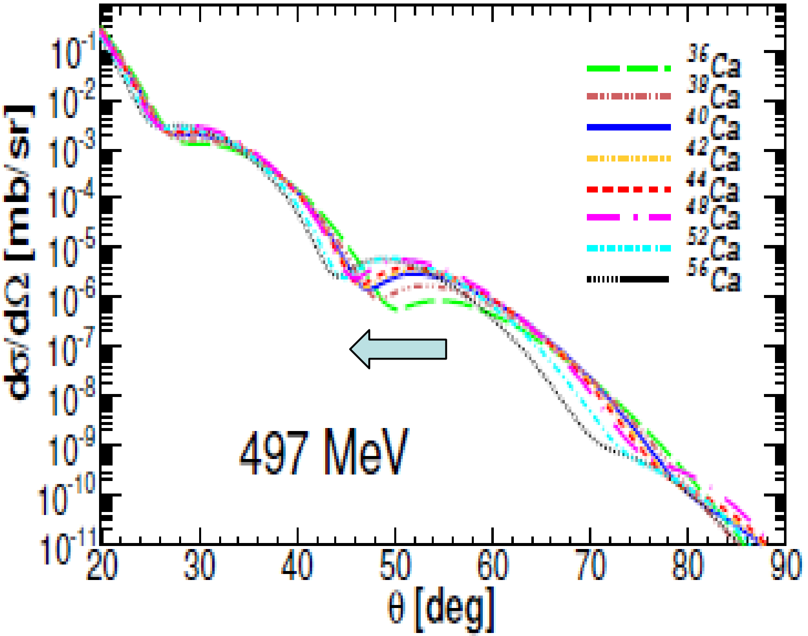

O isotopes

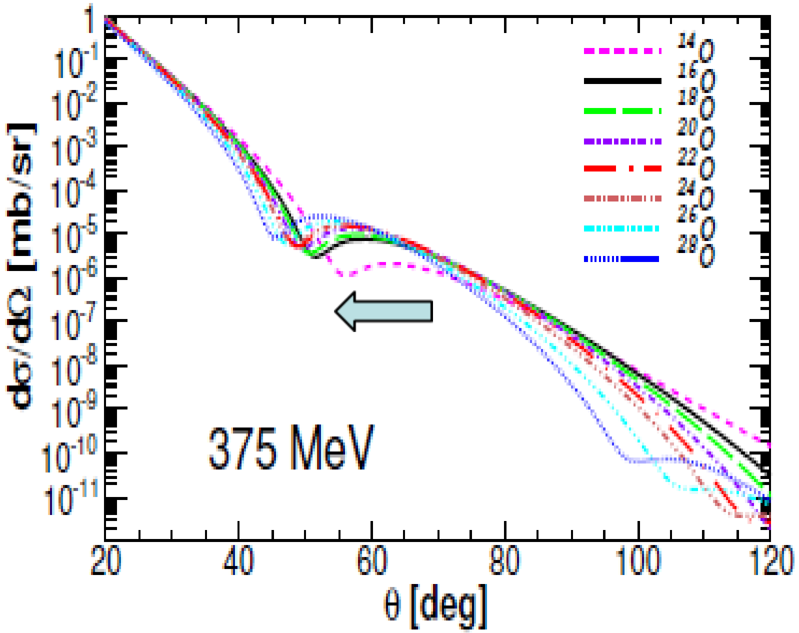

shift toward smaller angles

A. Meucci, M. Voraabi, C. Giusti, F.D. Pacati, P. Finelli, PRC 87 054620 (2013)

QE ELECTRON SCATTERING

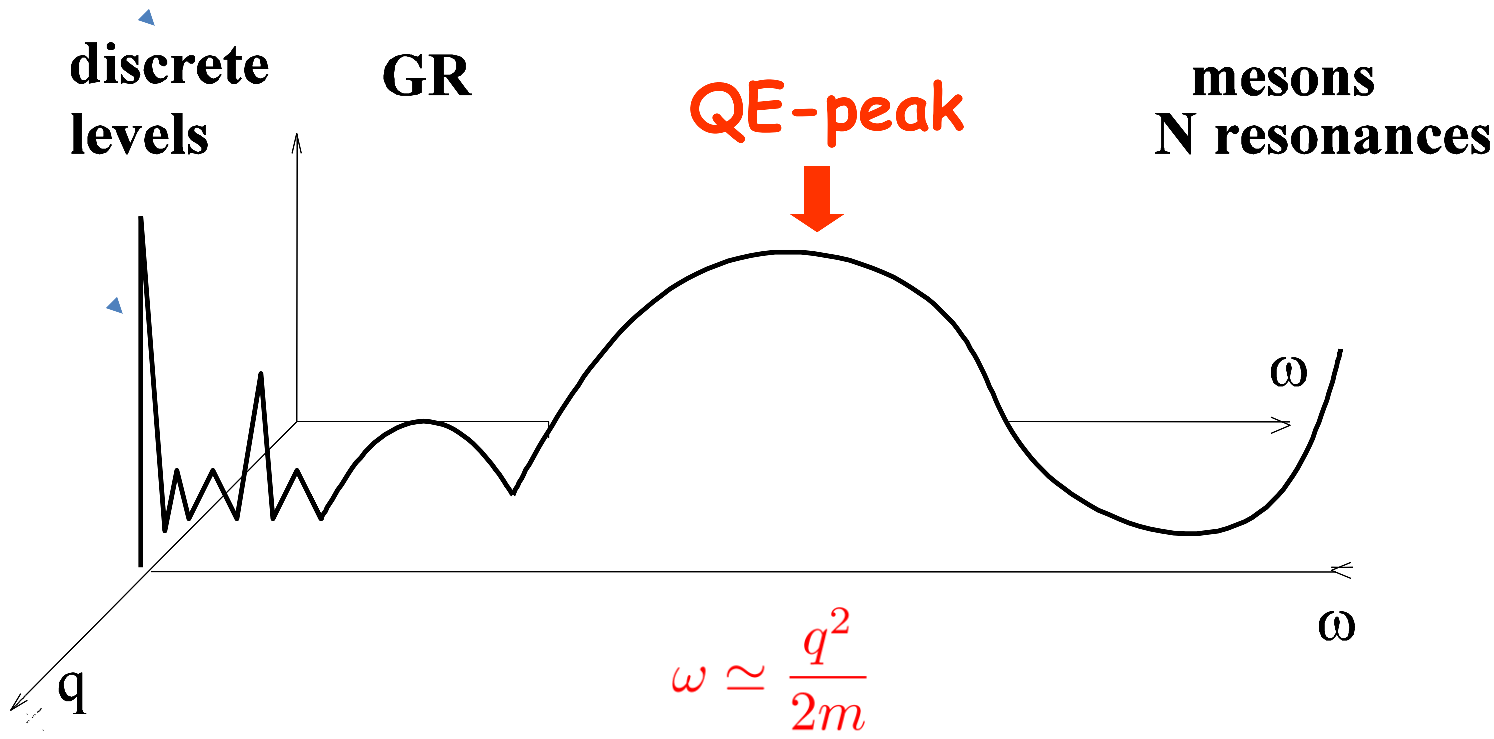

QE-peak dominated by one-nucleon knockout

QE ELECTRON SCATTERING

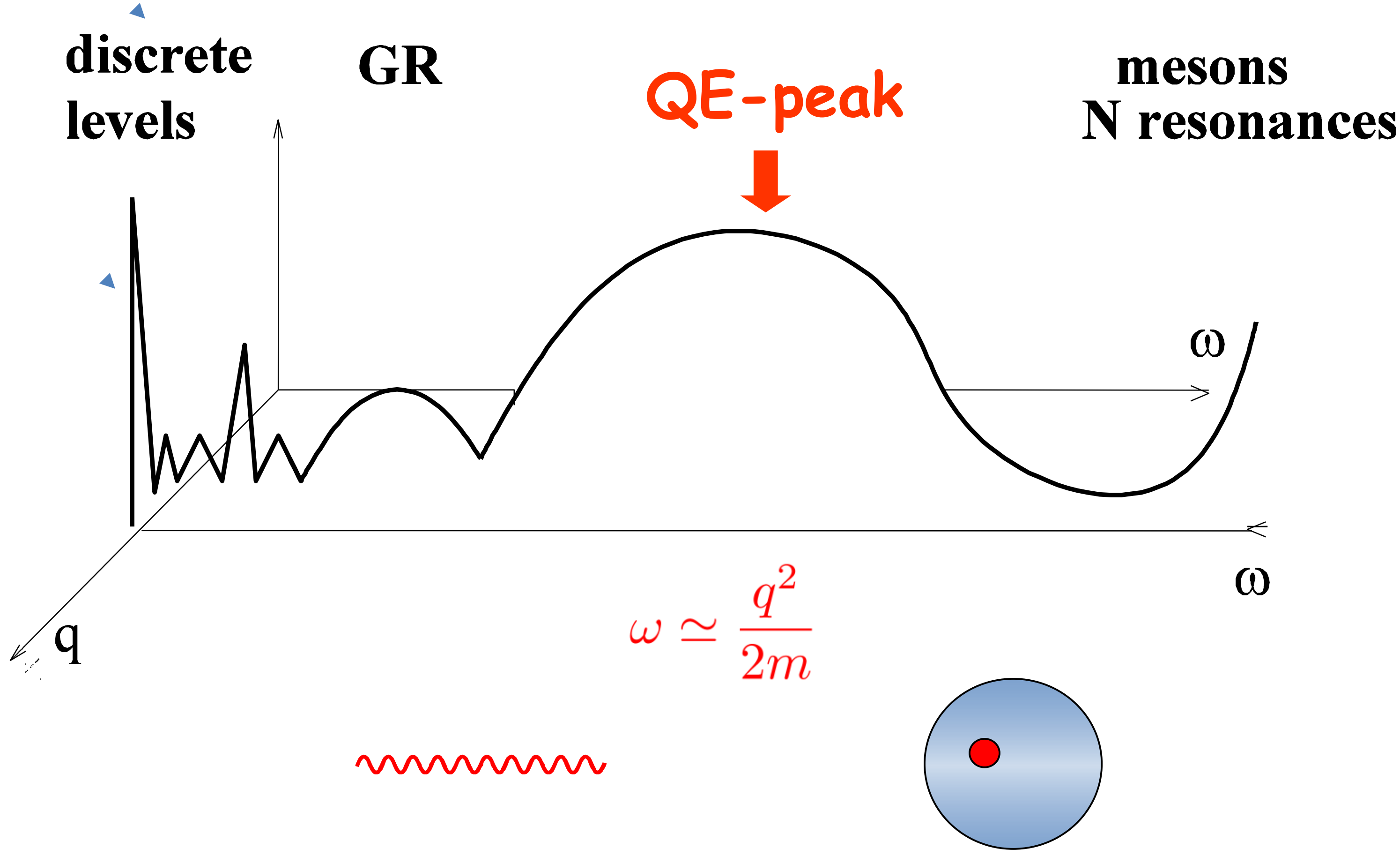

QE-peak dominated by one-nucleon knockout

QE ELECTRON SCATTERING

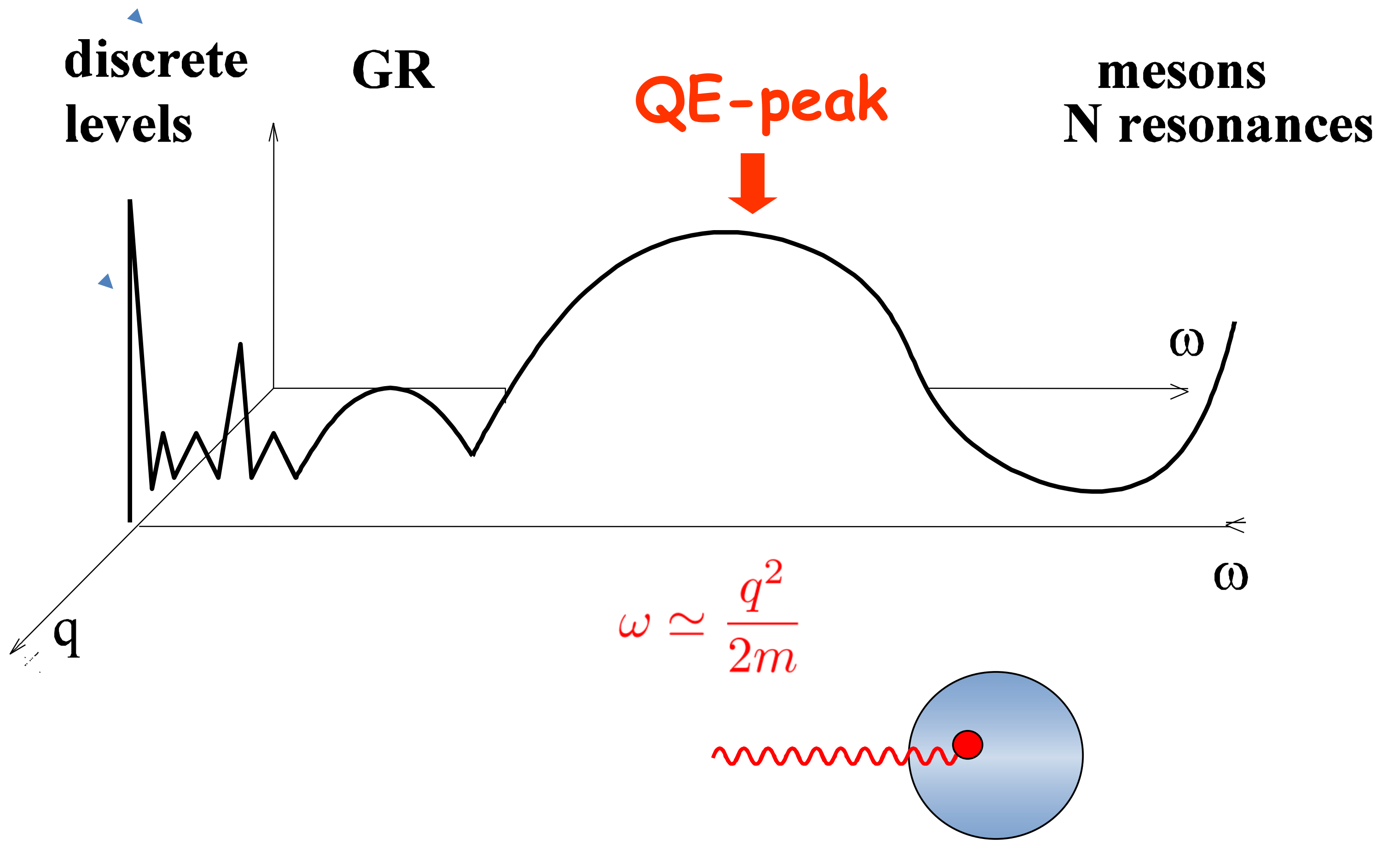

QE-peak dominated by one-nucleon knockout

QE ELECTRON SCATTERING

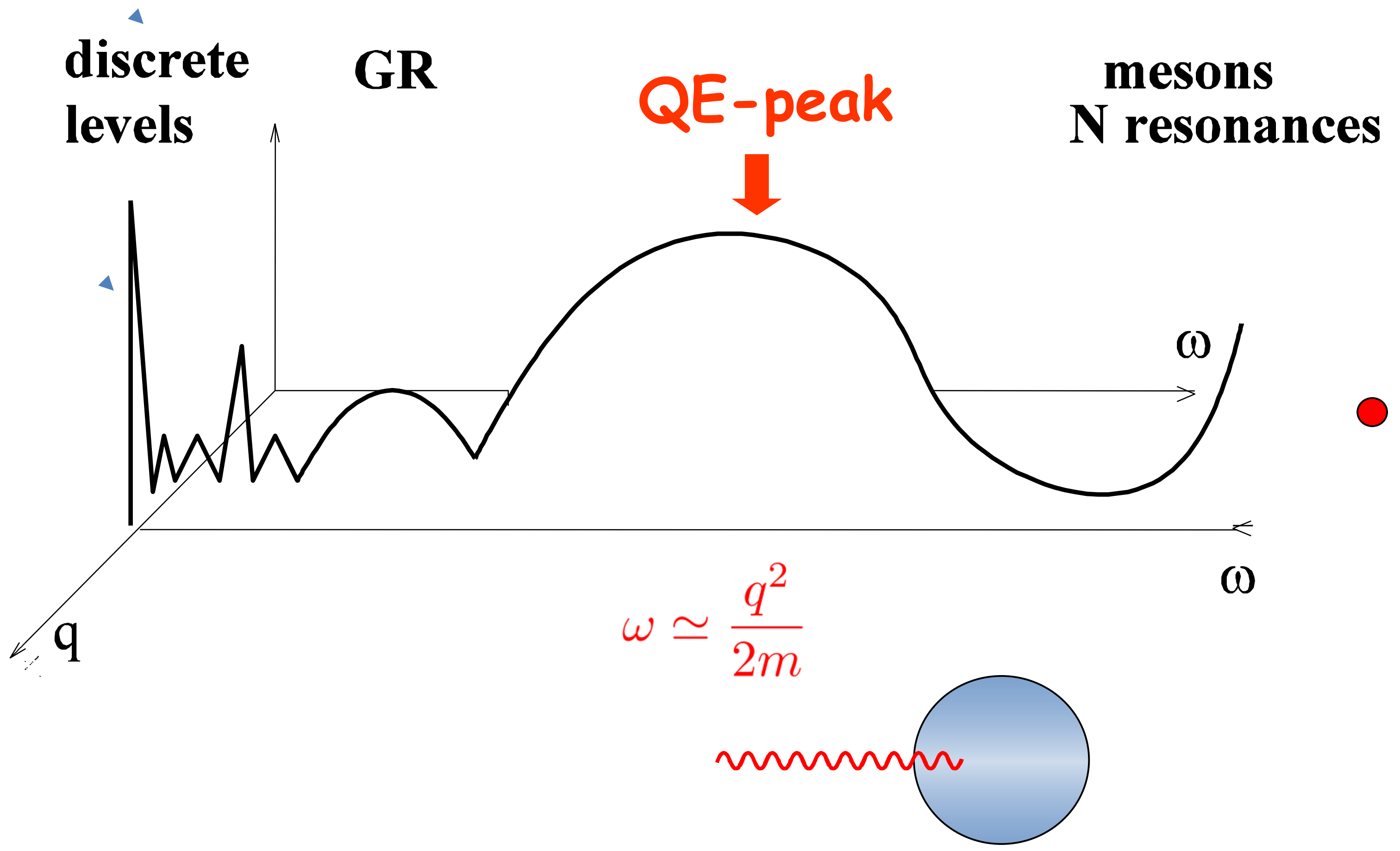

QE-peak dominated by one-nucleon knockout

QE

$$e + A \Longrightarrow e' + N + (A-1)$$

(e,e'p)

QE

$$e + A \Longrightarrow e' + N + (A-1)$$

1NKO

both e' and N detected (e,e'p)

(A-1) discrete eigenstate

exclusive (e,e'p)

proton-hole states

properties of bound protons

s.p. aspects of nuclear structure

validity and limitation of IPSM

nuclear correlations

EXCLUSIVE

(e,e'p) | QE | (e,e')

$$e + A \Longrightarrow e' + N + (A-1)$$

$$e + A \Longrightarrow e' + N + (A-1)$$

1NKO

both e' and N detected (e,e'p)

(A-1) discrete eigenstate

exclusive (e,e'p)

proton-hole states

properties of bound protons

s.p. aspects of nuclear structure

validity and limitation of IPSM

nuclear correlations

EXCLUSIVE

only e' detected

all final states included

discrete and continuum spectrum

less specific information more closely related to the dynamics of initial nuclear g.s.

width of QE peak direct measurement of average mom. of nucleons in nuclei, shape depends on the energy and momentum distribution of the bound nucleons

INCLUSIVE

OPEA

(e,e'p)

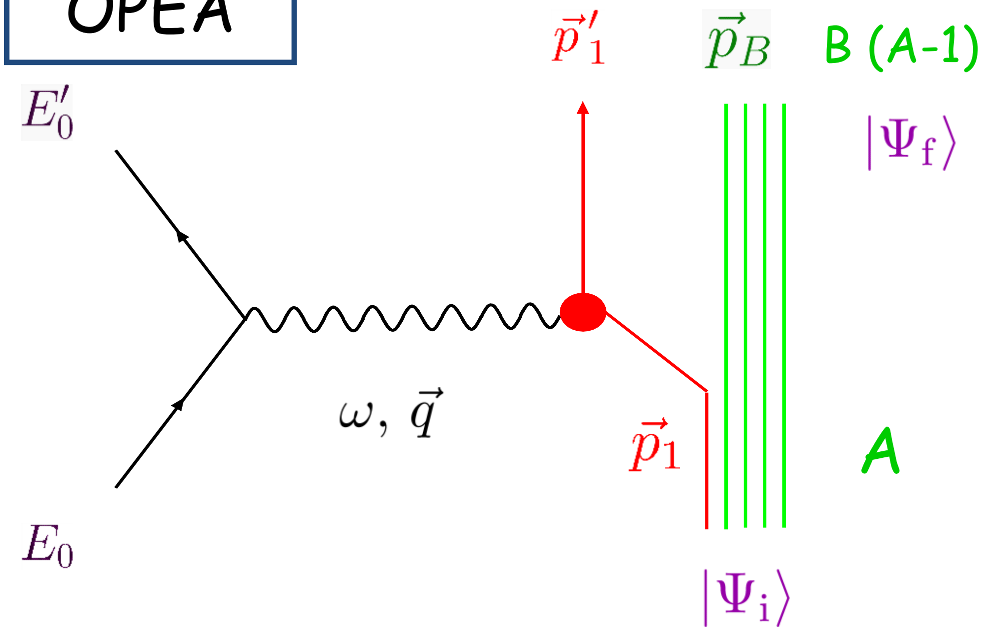

$$E_{\rm m} = \omega - \frac{{p'_1}^2}{2m} - \frac{{p_B}^2}{2m(A-1)} = W^*_B - W_A$$ missing energy

$$\vec{p}_{\rm m} = \vec{q} - \vec{p'}_1 = -\vec{p}_1 = \vec{p}_B$$ missing momentum

Experimental data: E_m and p_m distributions

$$^{16}\mathrm{O}(e,e'p)$$

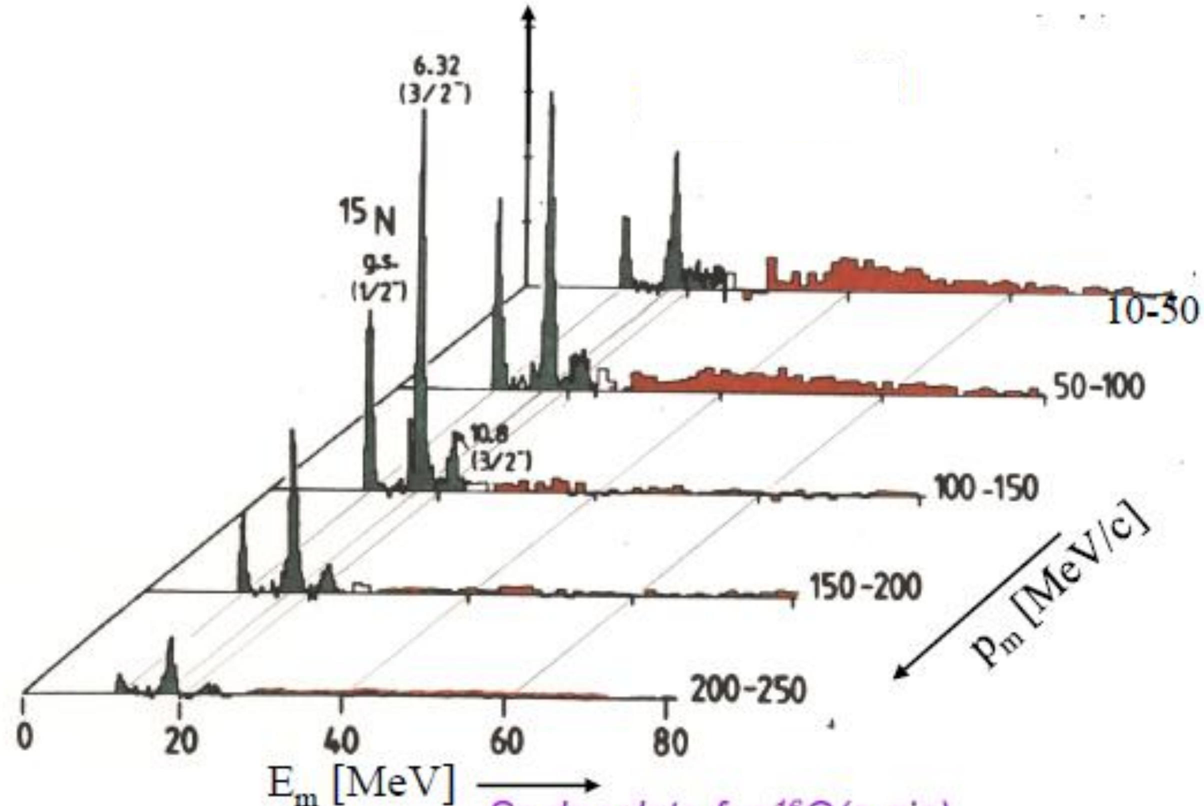

Saclay data for ^{16}O(e,e'p)

[Mougey et al., Nucl. Phys. A335, 35 (1980)]

Experimental data: E_m and p_m distributions

For E_m corresponding to a peak we assume that the residual nucleus is in a discrete eigenstate

$$^{16}\mathrm{O}(e,e'p)$$

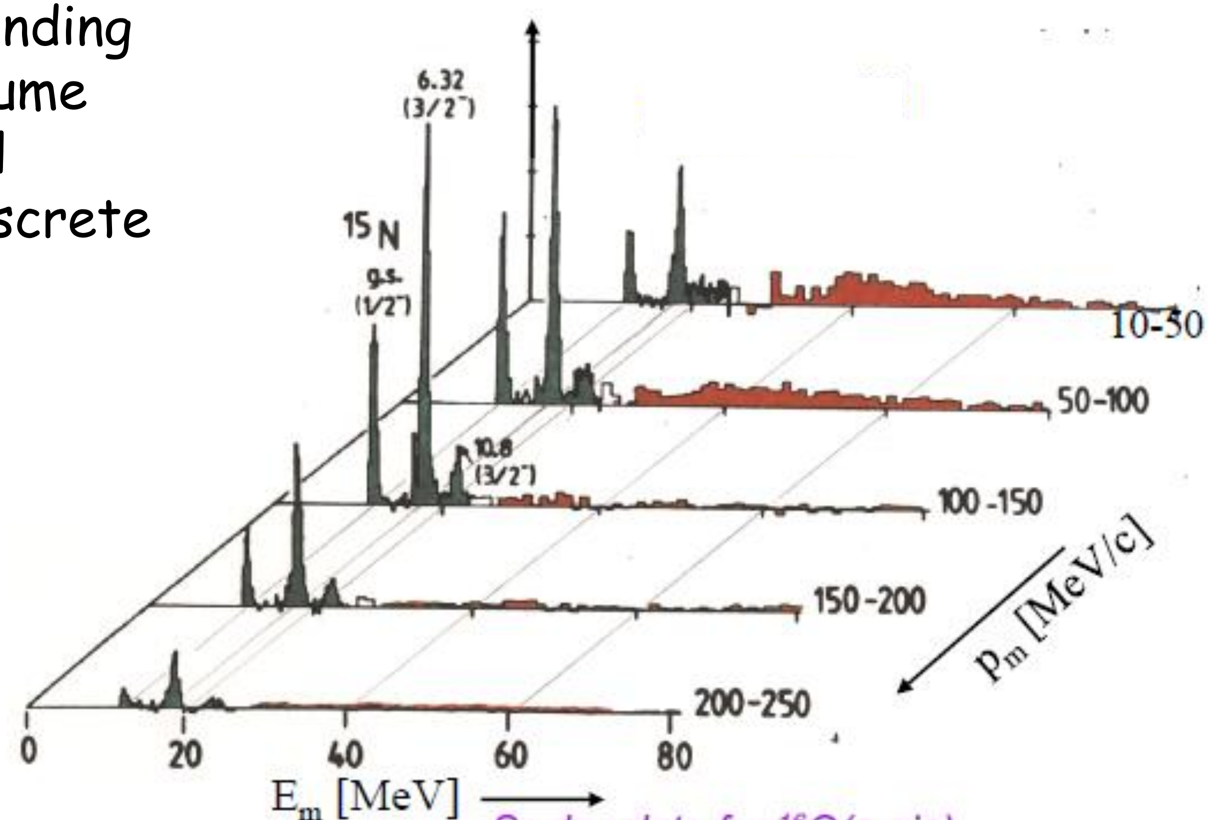

Saclay data for ^{16}O(e,e'p)

[Mougey et al., Nucl. Phys. A335, 35 (1980)]

E_m

exclusive reaction

ONE-HOLE SPECTRAL FUNCTION

$$S(\vec{p_1}, \vec{\bar{p}_1}; E_m) = \langle \Psi_{\mathrm{i}} | a^{+}_{\vec{\bar{p}}_1} \delta(E_m - H) a_{\vec{p_1}} | \Psi_{\mathrm{i}} \rangle$$

$$\vec{p}_1 = \vec{\bar{p}}_1$$

joint probability of removing from the target a nucleon p_1
leaving the residual nucleus in a state with energy E_m

E_m

exclusive reaction

ONE-HOLE SPECTRAL FUNCTION

$$S(\vec{p_1},\vec{\bar{p_1}};E_m) = \langle \Psi_\mathrm{i} | a^+_{\vec{\bar{p}}_1} \delta(E_m - H) a_{\vec{p_1}} | \Psi_\mathrm{i} \rangle$$

$\vec{p}_1 = \vec{\bar{p}}_1$

joint probability of removing from the target a nucleon p_1 leaving the residual nucleus in a state with energy E_m

$$\int S(\vec{p_1},\vec{\bar{p_1}};E_m)\mathrm{d}E_m = \boxed{\rho(\vec{p_1},\vec{\bar{p_1}})}$$

inclusive reaction : one-body density

$\vec{p}_1 = \vec{\bar{p}}_1 \Rightarrow \rho(\vec{p_1},\vec{\bar{p_1}}) = \boxed{F(\vec{p_1})}$

MOMENTUM DISTRIBUTION

$$F(\vec{p_1}) = \int |\Psi_\mathrm{i}(\vec{p_1},\vec{p_2},....,\vec{p_A}|^2 \mathrm{d}\vec{p_2}....\mathrm{d}\vec{p_A}$$

probability of finding in the target a nucleon with momentum p_1

OPEA

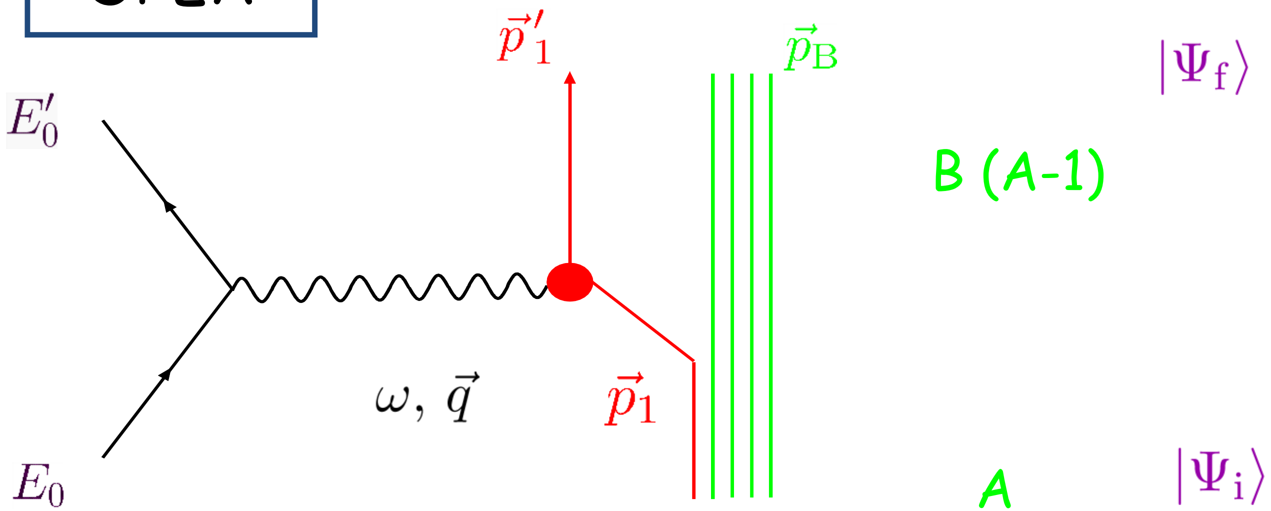

$$\sigma = K L^{\mu\nu}\ W_{\mu\nu}$$

OPEA

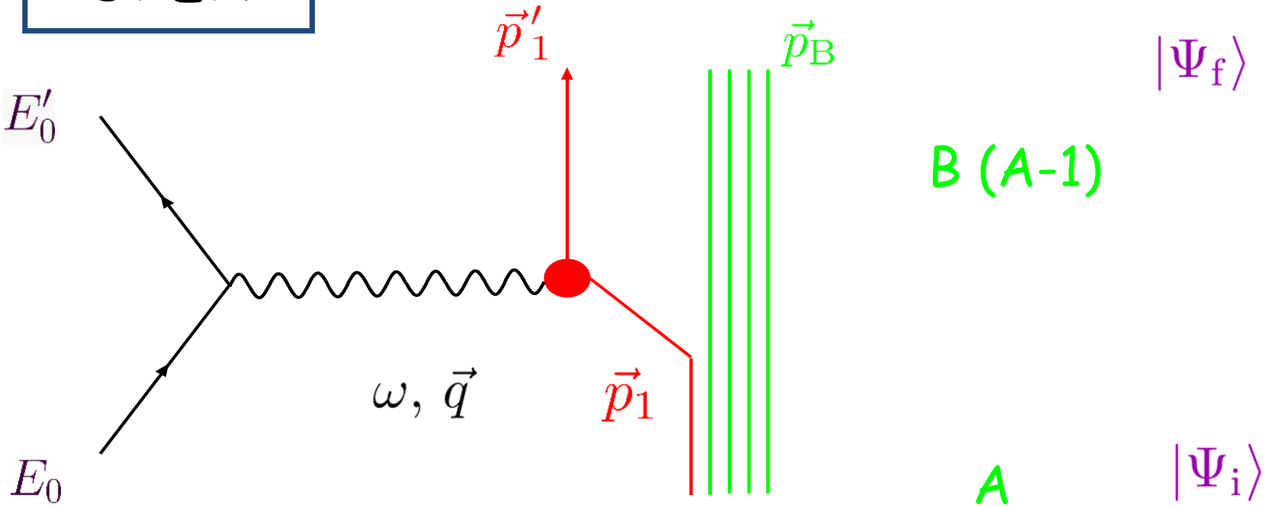

$$\sigma = K L^{\mu\nu}\ W_{\mu\nu}$$

lepton tensor

OPEA

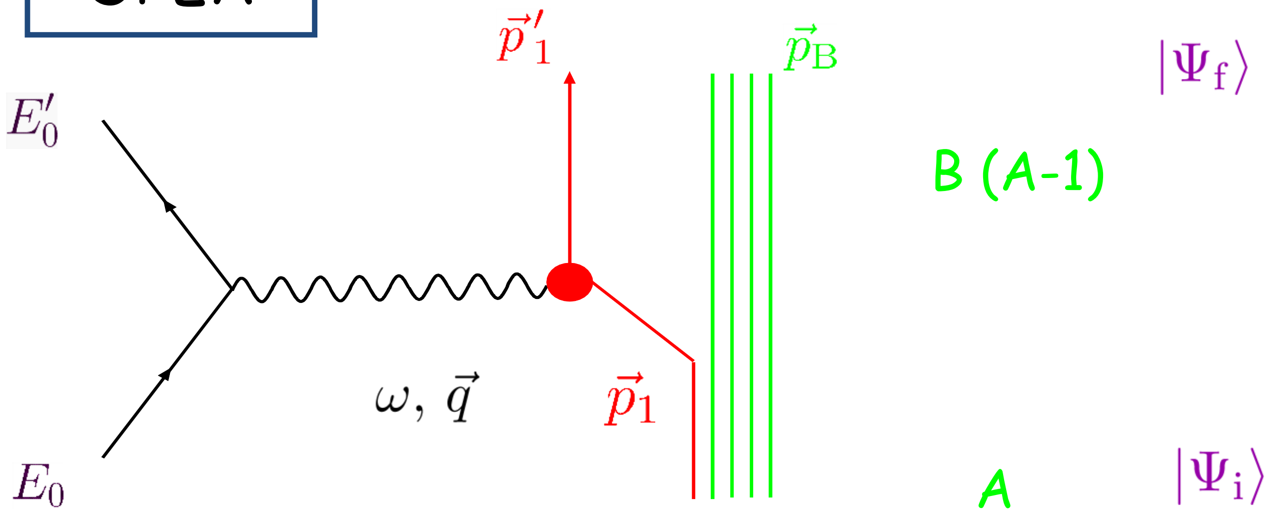

$$\sigma = K L^{\mu\nu}\ W_{\mu\nu}$$

hadron tensor

OPEA

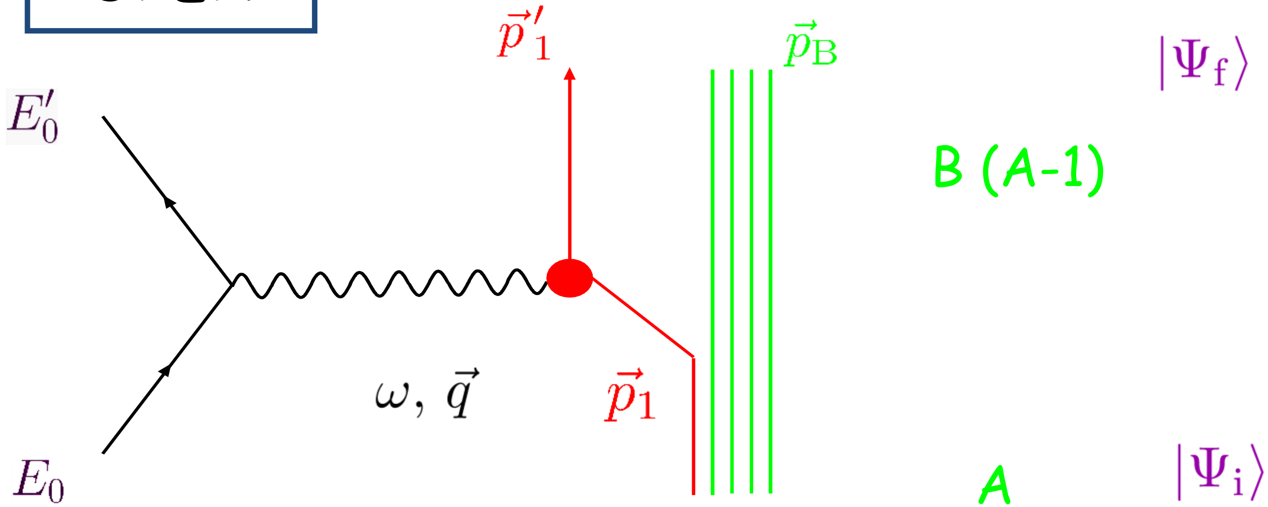

$$\sigma = K L^{\mu\nu}\ W_{\mu\nu}$$

hadron tensor

$$W^{\mu\nu} = \overline{\sum_{\mathrm{i,f}}} J^{\mu}(\vec{q}) J^{\nu *}(\vec{q}) \delta(E_{\mathrm{i}} - E_{\mathrm{f}})$$

$$J^{\mu}(\vec{q}) = \int \mathrm{e}^{\mathrm{i}\vec{q}\cdot\vec{r}} \langle \Psi_{\mathrm{f}} \mid \hat{J}^{\mu}(\vec{r}) \mid \Psi_{\mathrm{i}} \rangle \mathrm{d}\vec{r}$$

OPEA

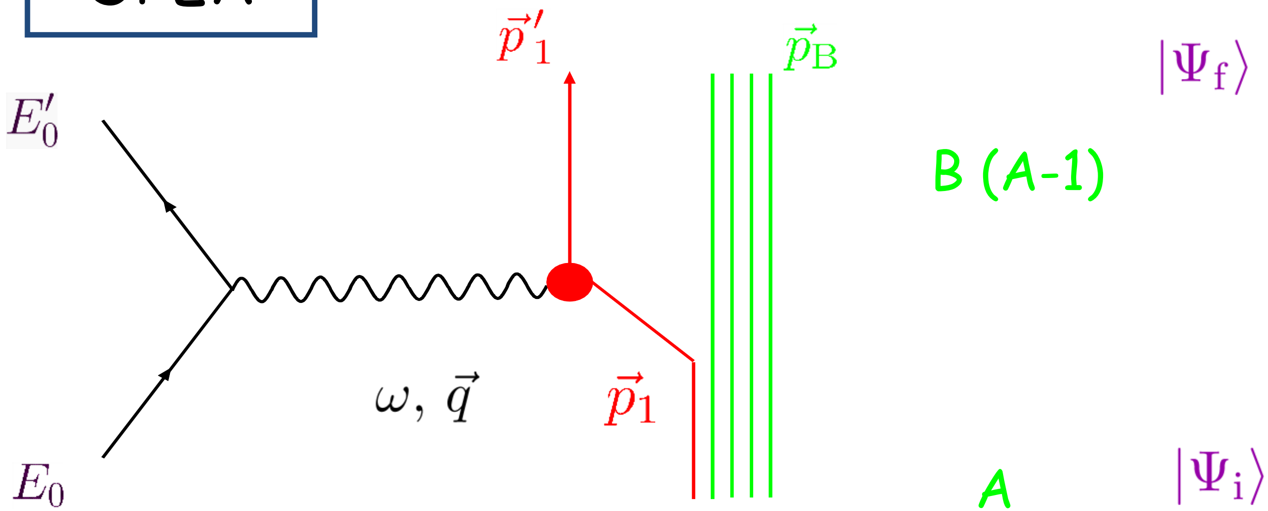

$$\sigma = K L^{\mu\nu}\ W_{\mu\nu}$$

hadron tensor

$$W^{\mu\nu} = \overline{\sum_{i,f}} J^{\mu}(\vec{q}) J^{\nu *}(\vec{q}) \delta(E_i - E_f)$$

$$J^{\mu}(\vec{q}) = \int e^{i\vec{q}\cdot\vec{r}} \langle \Psi_f \mid \hat{J}^{\mu}(\vec{r}) \mid \Psi_i \rangle d\vec{r}$$

(e,e′p)

- exclusive reaction n
- DKO mechanism: the probe interacts through a one-body current with one nucleon which is then emitted the remaining nucleons are spectators
- impulse approximation IA

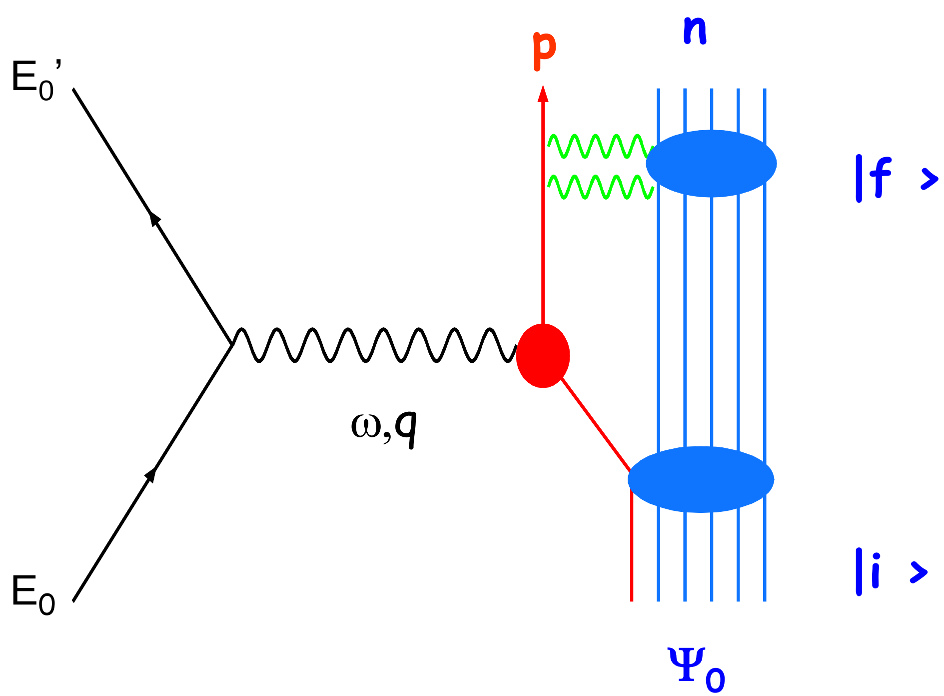

(e,e'p)

- exclusive reaction n
- DKO mechanism: the probe interacts through a one-body current with one nucleon which is then emitted the remaining nucleons are spectators
- impulse approximation IA

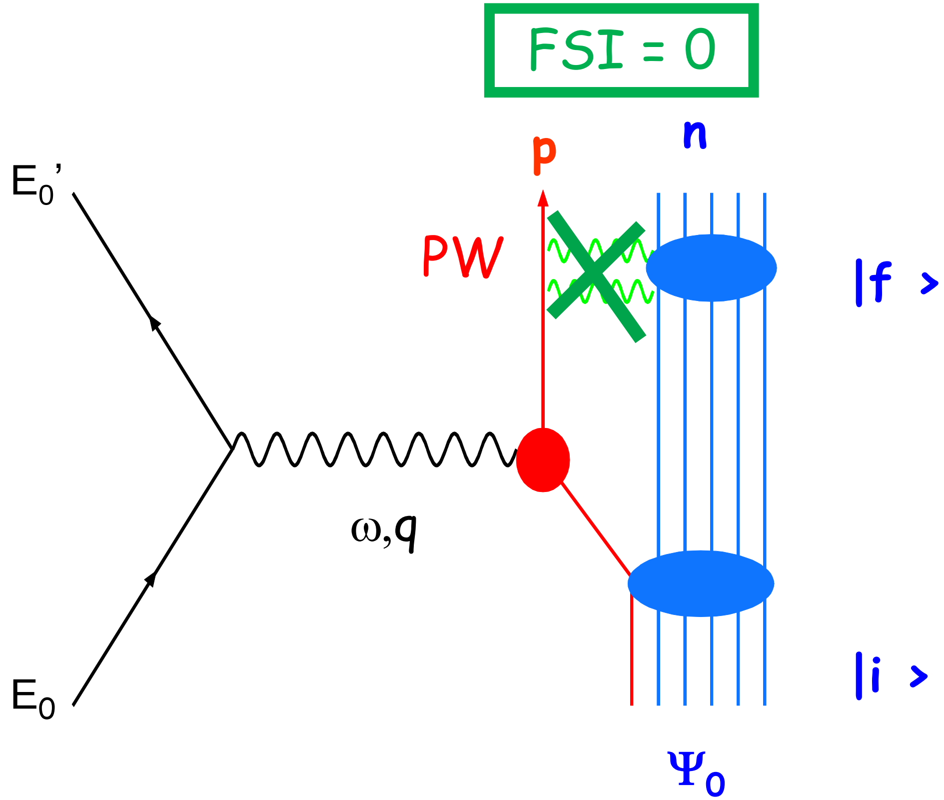

FSI=0

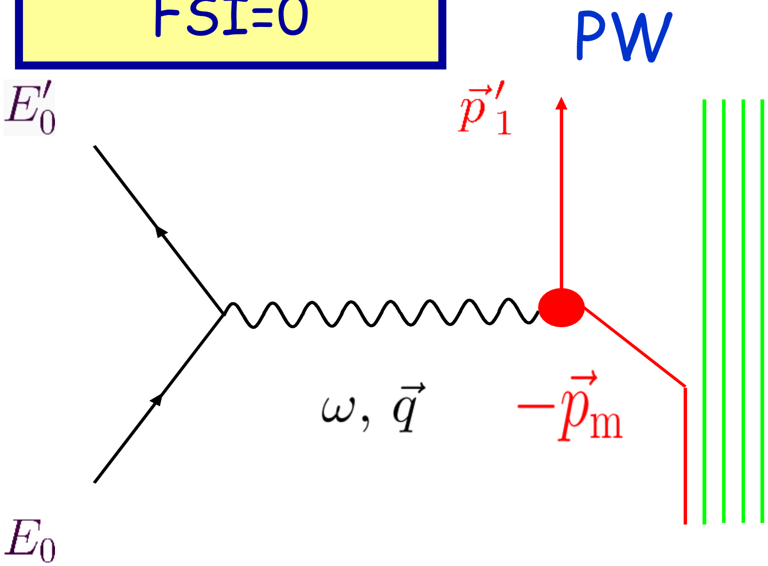

PLANE-WAVE IMPULSE APPROXIMATION

PWIA

factorized cross section

$$\sigma = K\ \sigma_{\rm ep}\ \ S(E_{\rm m}, -\vec{p}_{\rm m})$$

spectral function

$$S(E_{\rm m}, -\vec{p}_{\rm m}) = \sum_n\ \lambda_n(E_{\rm m})\ \ |\phi_n(-\vec{p}_{\rm m})|^2$$

spectroscopic factor

overlap function

$$S(E_{\rm m}, -\vec{p}_{\rm m}) = \sum_n \underbrace{\lambda_n(E_{\rm m})}_{\text{spectroscopic factor}} \; \underbrace{|\phi_n(-\vec{p}_{\rm m})|^2}_{\text{overlap function}}$$

For each E_m the mom. dependence of the SF is given by the mom. distr. of the quasi-hole states n produced in the target nucleus at that energy and described by the normalized OF

The norm of the OF, the spectroscopic factor gives the probability that n is a pure hole state in the target.

IPSM

ϕ_n s.p. SM state

λ_n 1 occupied SM states

0 empty SM states

There are correlations and the strength of the quasi-hole state is fragmented over a set of s.p. states $0 \leq \lambda_n \leq 1$

DWIA (e,e'p)

- exclusive reaction n
- DKO IA
- FSI DWIA
- unfactorized c.s.
- non diagonal SF

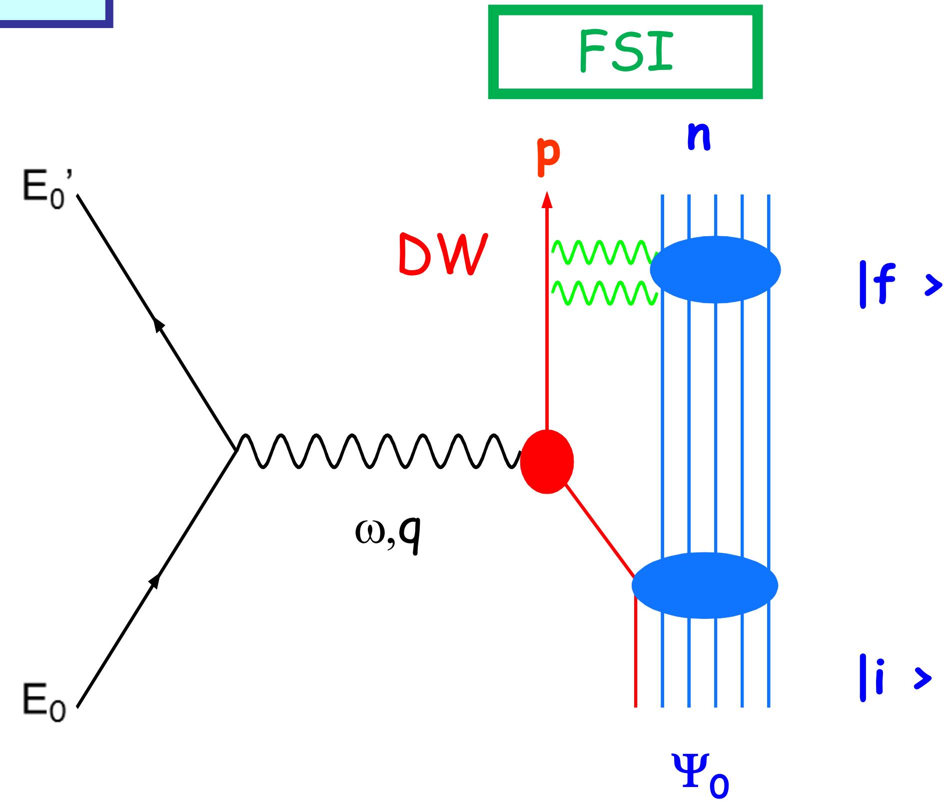

$$\langle f \mid J^\mu(\boldsymbol{q}) \mid i \rangle \Rightarrow \lambda_n^{1/2} \langle \chi_{\boldsymbol{p}}^{(-)} \mid j^\mu(\boldsymbol{q}) \mid \phi_n \rangle$$

Direct knockout DWIA (e,e′p)

$$\lambda_n^{1/2} \ \langle \chi^{(-)} \mid j^{\mu} \mid \phi_n \rangle$$

- j^{μ} one-body nuclear current
- $\chi^{(-)}$ s.p. scattering w.f. $H^{+}(\omega+E_m)$
- ϕ_n s.p. bound state overlap function $H(-E_m)$
- λ_n spectroscopic factor
- $\chi^{(-)}$ and ϕ consistently derived as eigenfunctions of a Feshbach optical model Hamiltonian

DWIA-RDWIA calculations

- phenomenological ingredients usually adopted
- $\chi^{(-)}$ phenomenological optical potential
- ϕ_n phenomenological s.p. wave functions WS, HF MF (some calculations including correlations are available)
- nonrelativistic (DWIA) relativistic (RDWIA) ingredients
- λ_n extracted in comparison with data: reduction factor applied to the calculated c.s. to reproduce the magnitude of the experimental c.s.

DWIA-RDWIA calculations

- phenomenological ingredients usually adopted
- $\chi^{(-)}$ phenomenological optical potential
- ϕ_n phenomenological s.p. wave functions WS, HF MF (some calculations including correlations are available)
- nonrelativistic (DWIA) relativistic (RDWIA) ingredients
- λ_n extracted in comparison with data: reduction factor applied to the calculated c.s. to reproduce the magnitude of the experimental c.s.

DWIA and RDWIA: excellent description of (e,e′p) data

Experimental data: p_m distributions

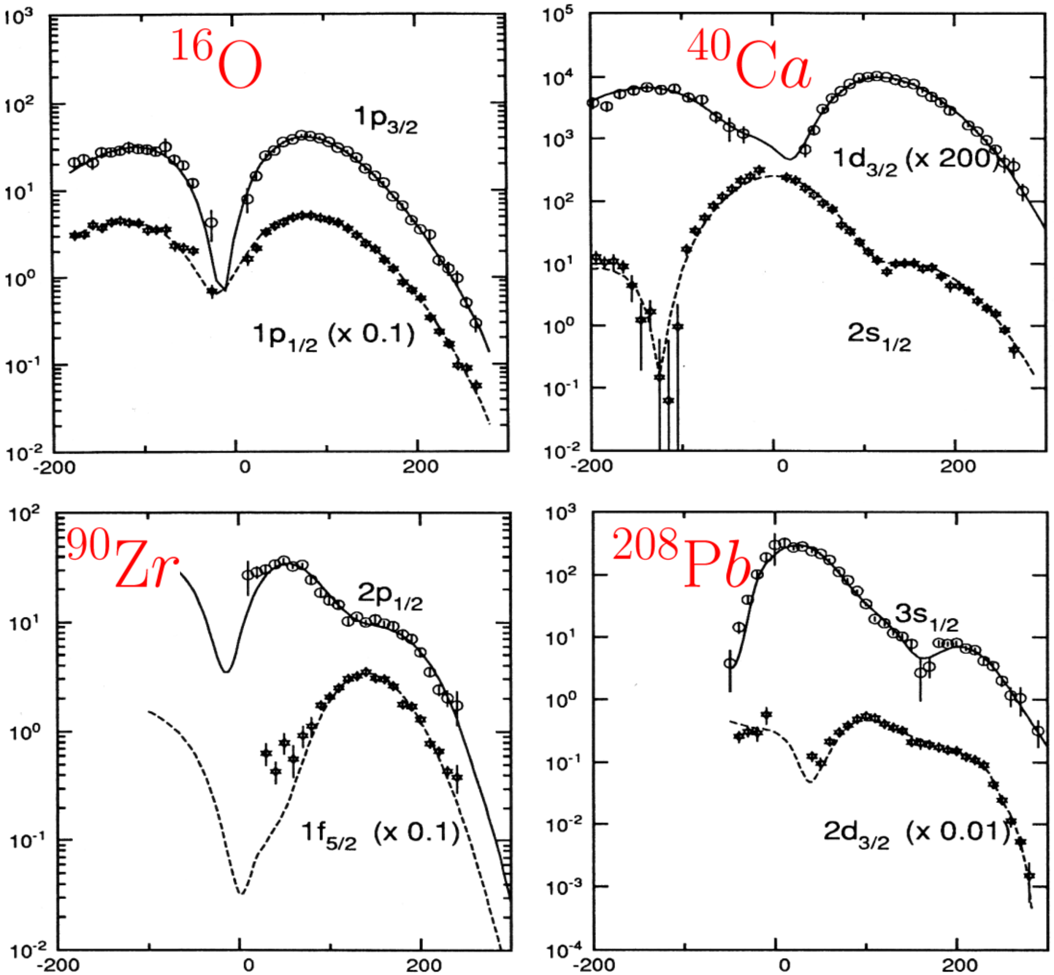

NIKHEF data & CDWIA calculations

Experimental data: p_m distributions

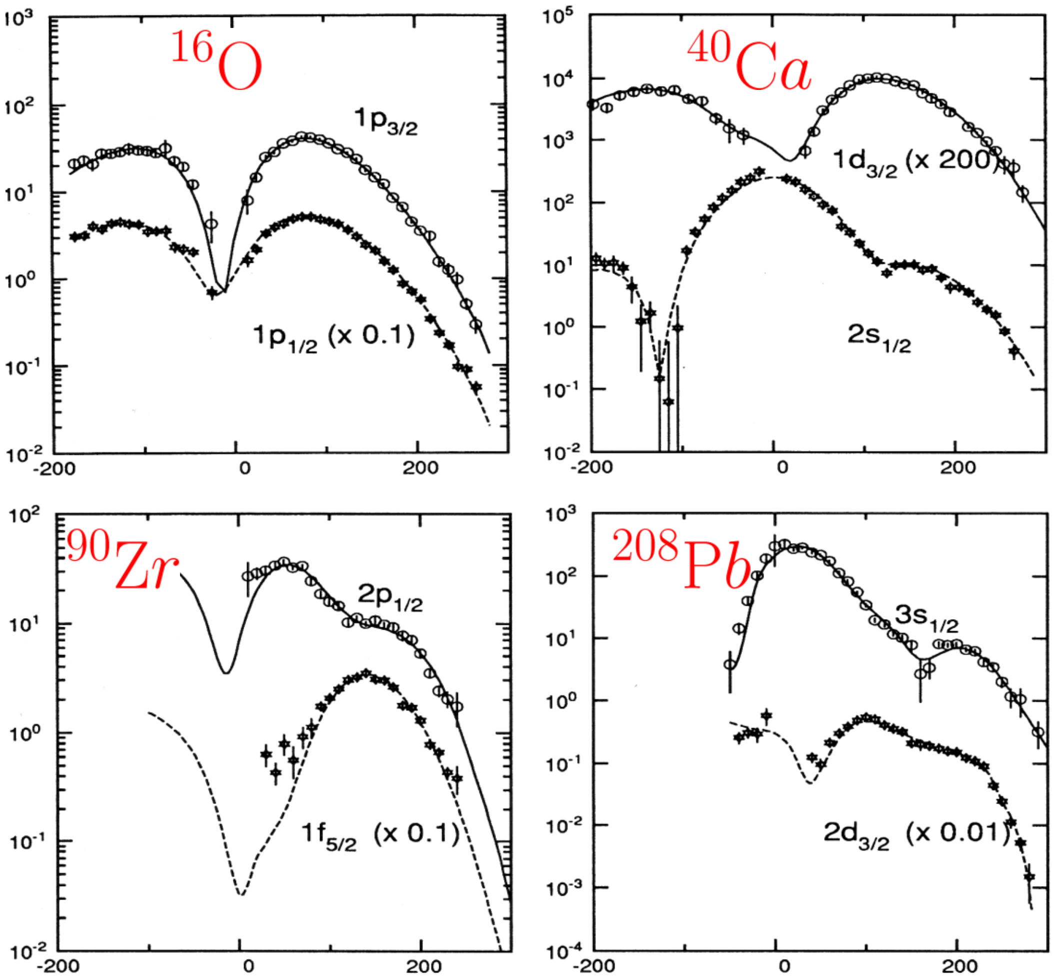

reduction factors applied:
spectroscopic factors

0.6 - 0.7

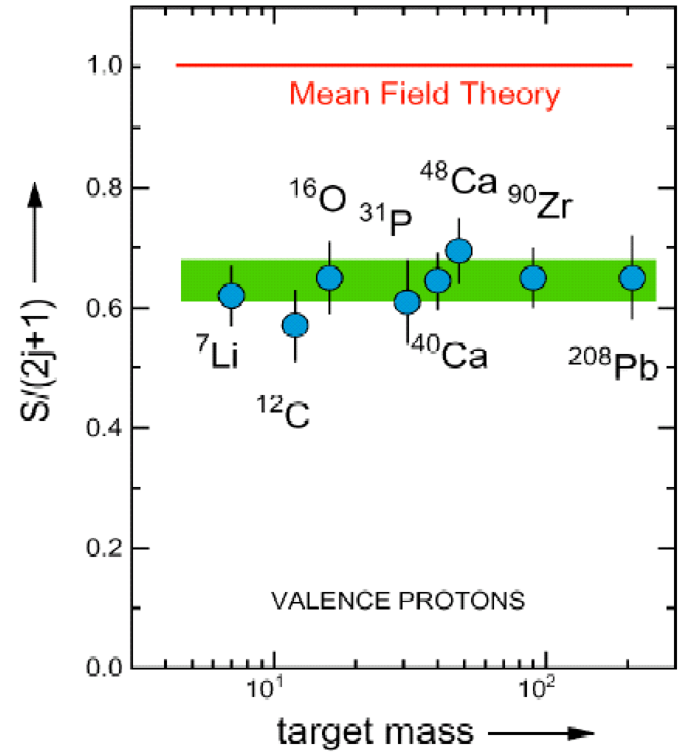

NIKHEF data & CDWIA calculations

Relativistic RDWIA

$^{16}O(e,e'p)$

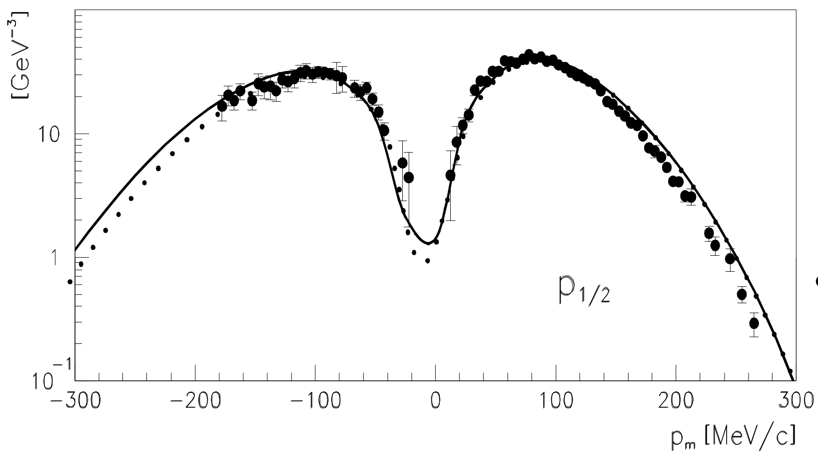

NIKHEF parallel kin E_0 = 520 MeV T_p = 90 MeV

rel RDWIA

nonrel DWIA

Relativistic RDWIA

$^{16}O(e,e'p)$

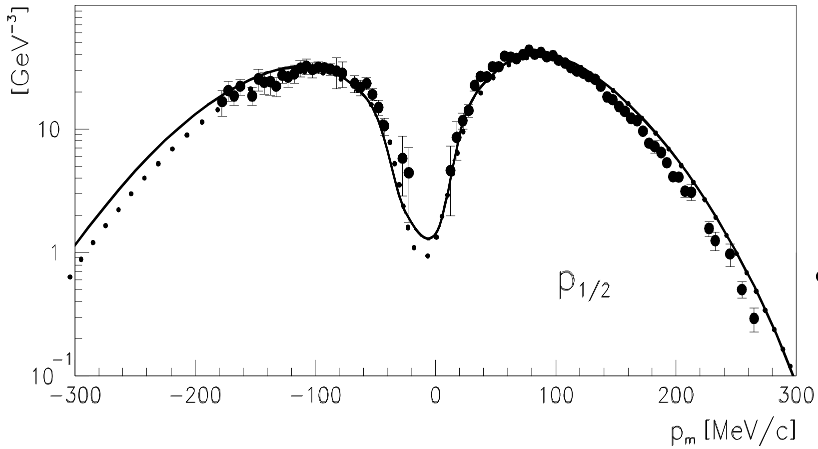

NIKHEF parallel kin $E_0 = 520$ MeV $T_p = 90$ MeV

rel RDWIA $\lambda_n = 0.7$

nonrel DWIA $\lambda_n = 0.65$

Relativistic RDWIA

$^{16}O(e,e'p)$

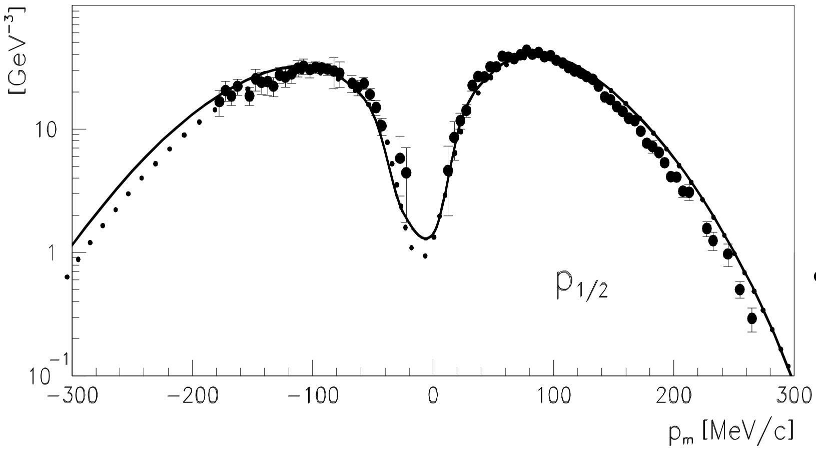

NIKHEF parallel kin E_0 = 520 MeV T_p = 90 MeV

rel RDWIA $\lambda_n = 0.7$

nonrel DWIA $\lambda_n = 0.65$

JLab (ω,q) const kin E_0 = 2445 MeV ω =439 MeV T_p= 435 MeV

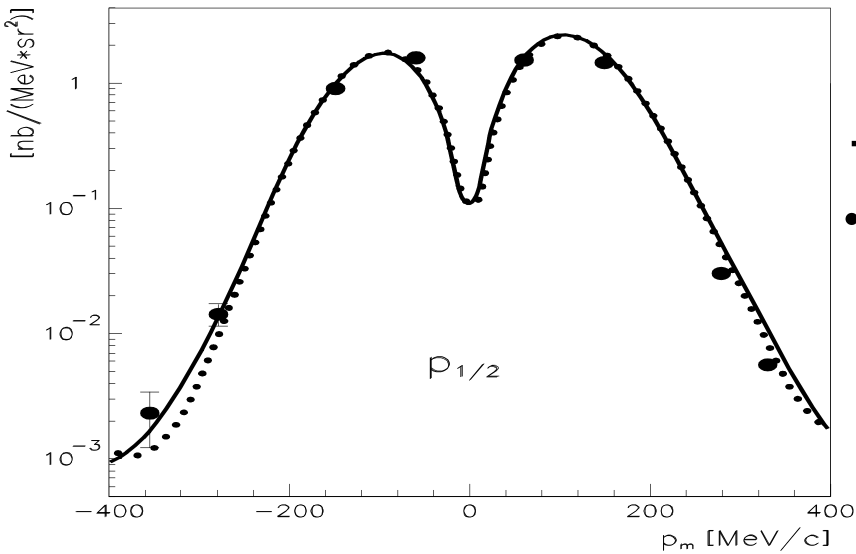

RDWIA diff opt.pot. $\lambda_n = 0.7$

Relativistic RDWIA

$^{16}O(e,e'p)$

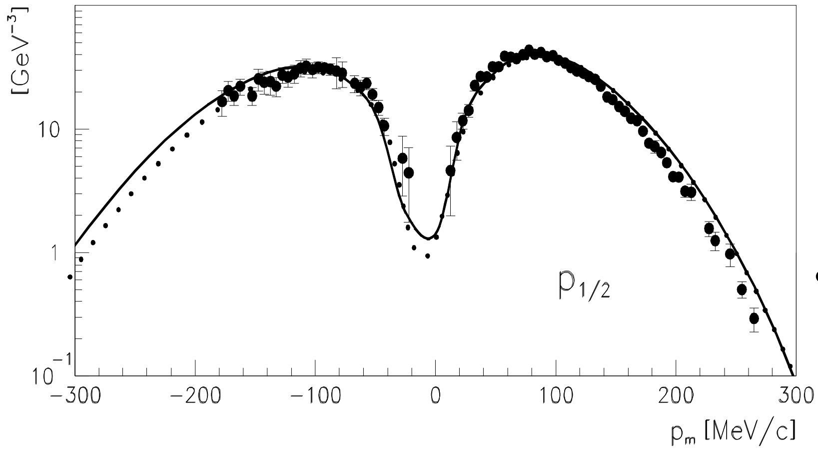

NIKHEF parallel kin E_0 = 520 MeV T_p = 90 MeV

rel RDWIA $\lambda_n = 0.7$

nonrel DWIA $\lambda_n = 0.65$

JLab (ω,q) const kin E_0 = 2445 MeV ω =439 MeV T_p= 435 MeV

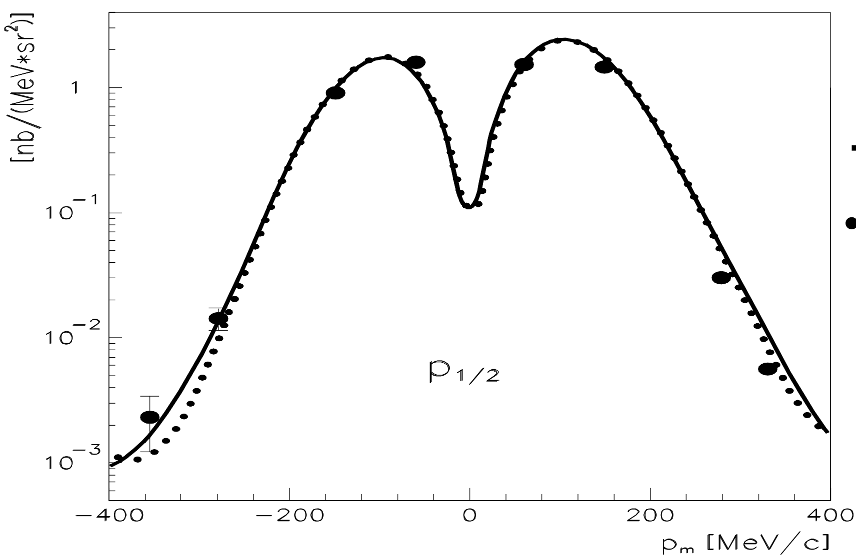

RDWIA diff opt.pot. $\lambda_n = 0.7$

$^{40}Ca(e,e'p)$

DWIA WS wave function

$1d_{3/2}$

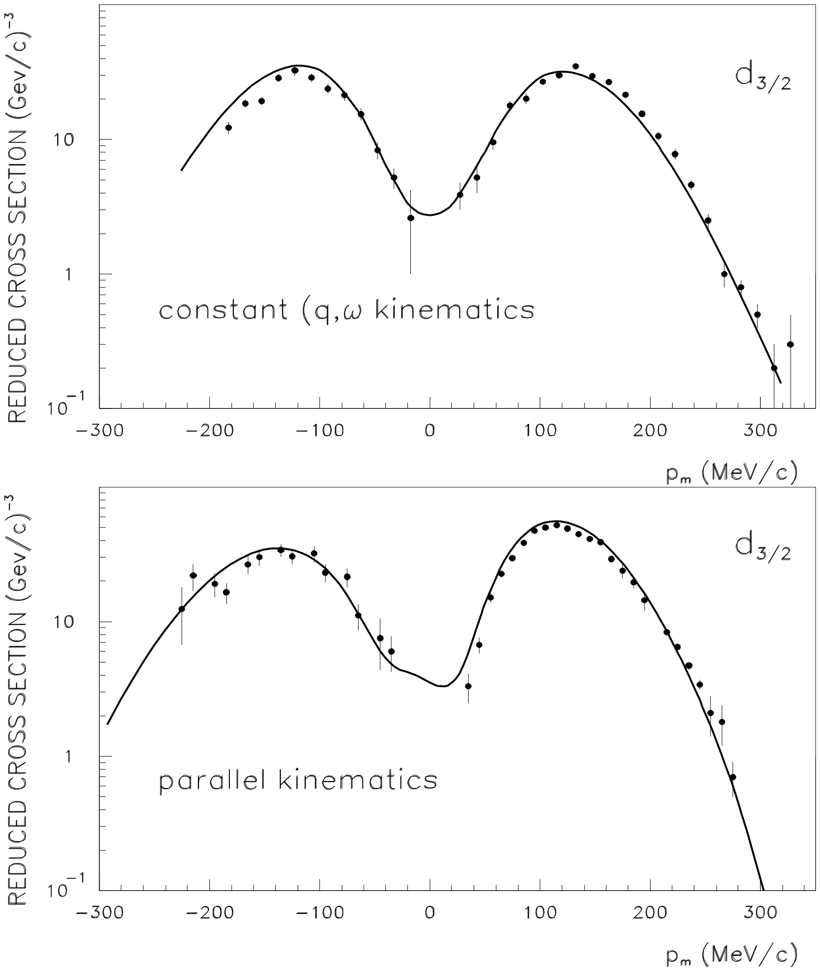

(ω,q) const: E_0=483.2 MeV θ =61.52 deg. q=450 MeV/c T_p=100 MeV

parallel kin: E_0=483.2 MeV T_p=100 MeV

NIKHEF data G.J. Kramer Ph. D. Thesis (1990)

$^{40}Ca(e,e'p)$

DWIA WS wave function

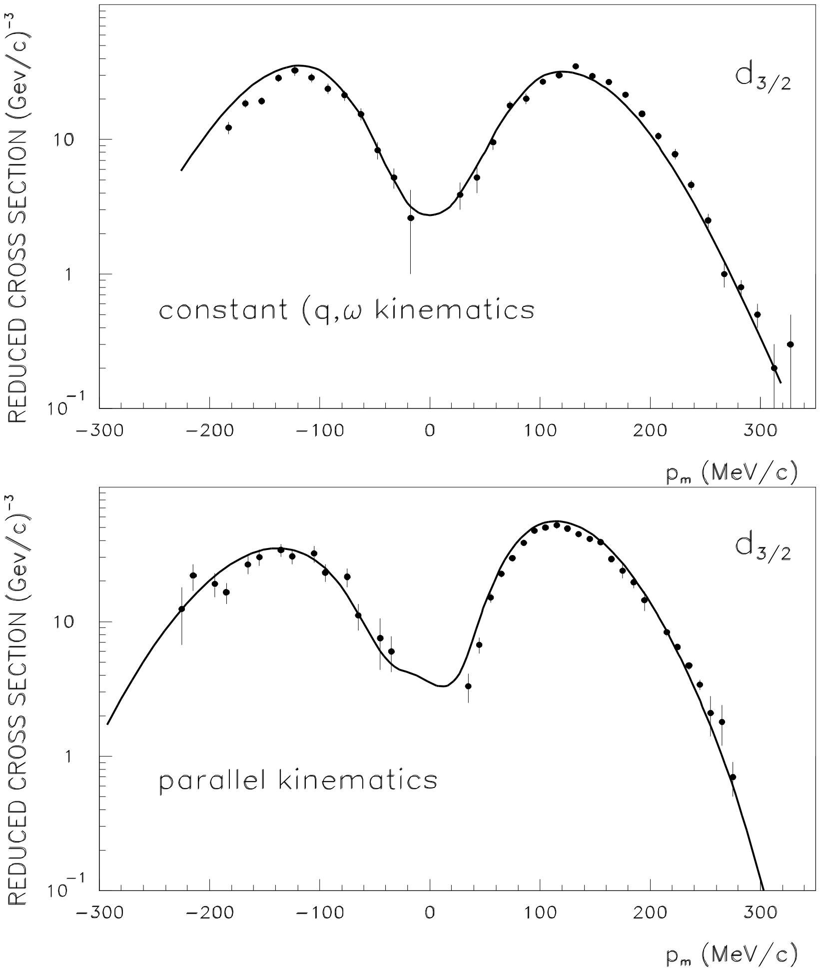

λ_n = 0.49

λ_n = 0.65

$1d_{3/2}$

(ω,q) const: E_0=483.2 MeV θ =61.52 deg. q=450 MeV/c T_p=100 MeV

parallel kin: E_0=483.2 MeV T_p=100 MeV

NIKHEF data G.J. Kramer Ph. D. Thesis (1990)

$^{40}Ca(e,e'p)$

DWIA WS wave function

$^{48}Ca(e,e'p)$

$1d_{3/2}$

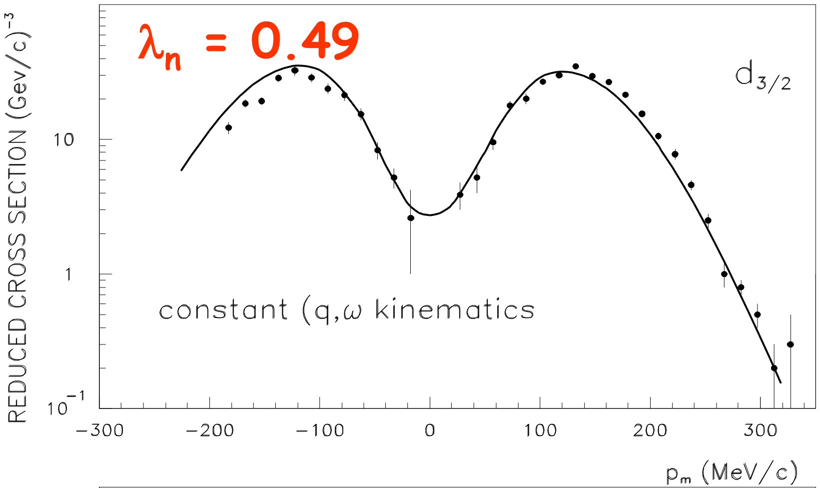

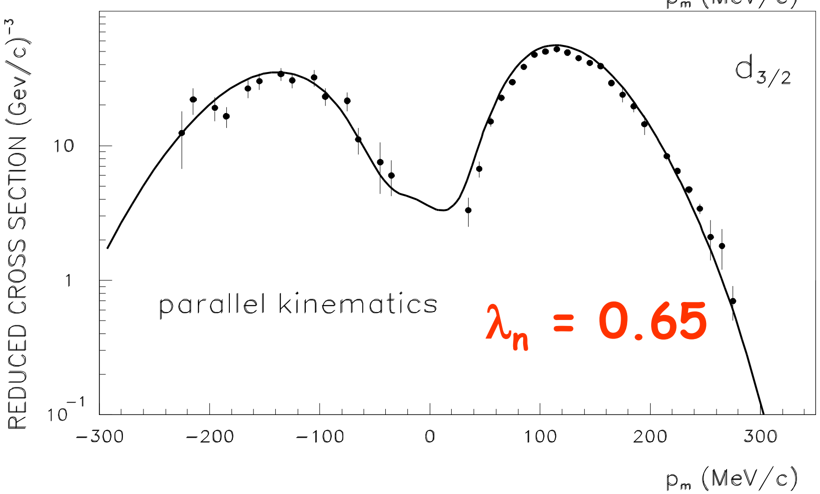

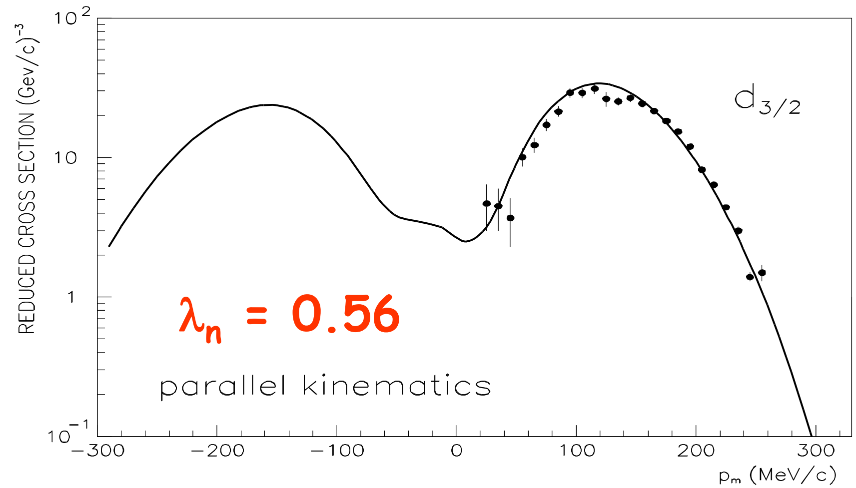

(ω,q) const: E_0=483.2 MeV θ =61.52 deg. q=450 MeV/c T_p=100 MeV

parallel kin: E_0=483.2 MeV T_p=100 MeV

NIKHEF data G.J. Kramer Ph. D. Thesis (1990)

$^{40}Ca(e,e'p)$

$^{48}Ca(e,e'p)$

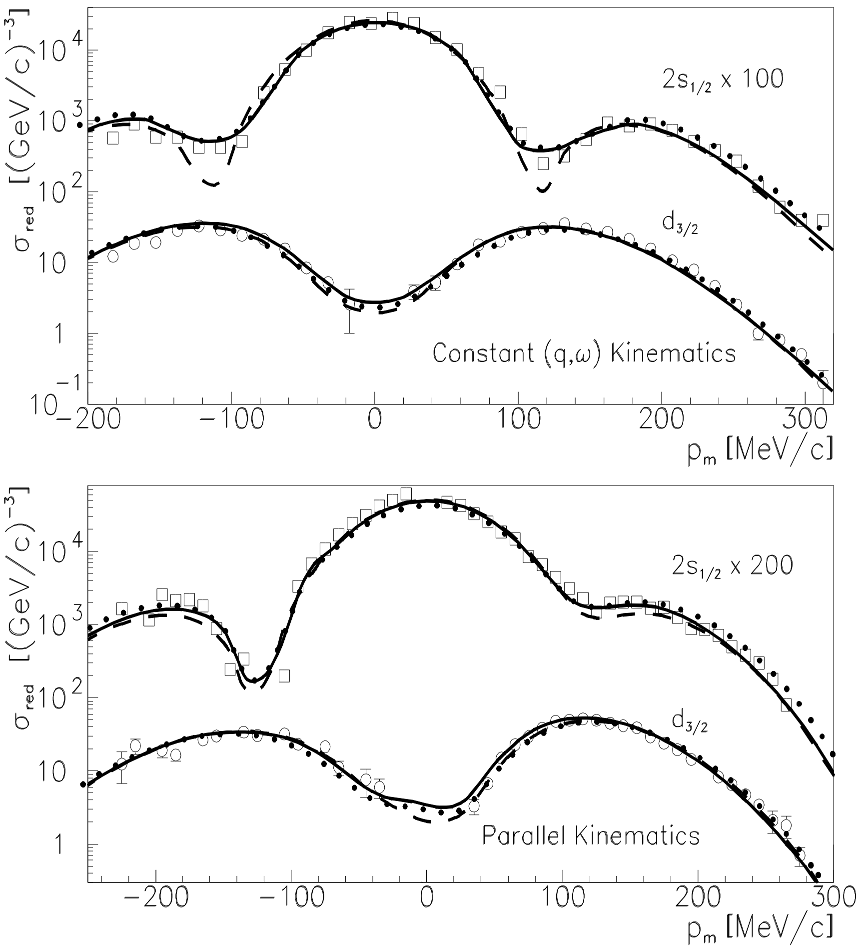

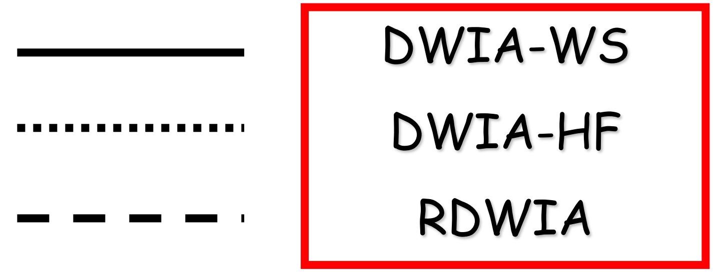

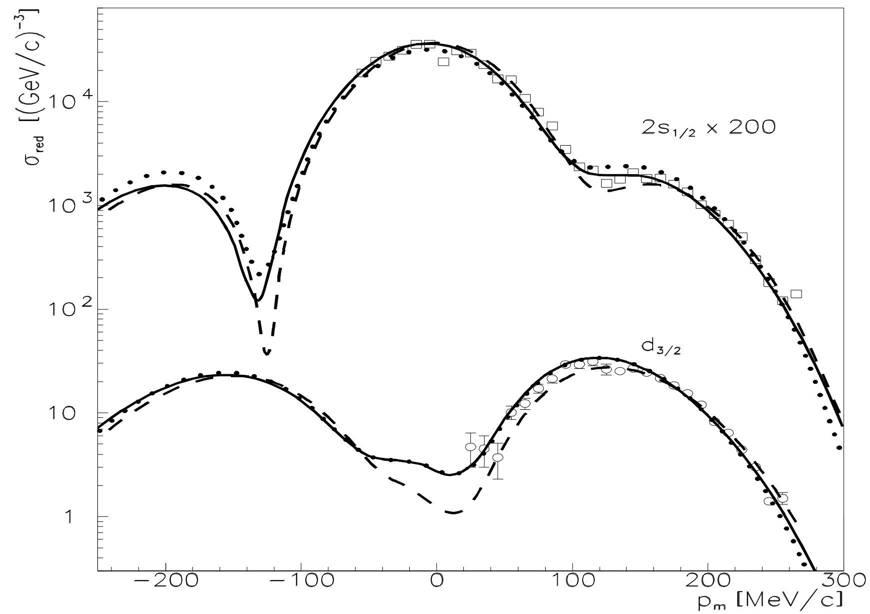

C.Giusti et al. PRC 024615 (2011)

$^{40}Ca(e,e'p)$

$1d_{3/2}$

$^{48}Ca(e,e'p)$

λ_n = 0.49 DWIA-WS

0.51 DWIA-HF

0.49 RDWIA

(ω,q) const kin

λ_n = 0.65 DWIA-WS

0.64 DWIA-HF

0.69 RDWIA

parallel kin

λ_n = 0.56 DWIA-WS

0.55 DWIA-HF

0.52 RDWIA

$^{40,48,52,60}Ca(e,e'p)$

- DWIA-WS DWIA-HF and RDWIA for Ca isotopes
- even-even isotopes, spherical nuclei where the s.p. levels are fully occupied and pairing effects should be minimized

$^{40,48,52,60}Ca(e,e'p)$

$d_{3/2}$

40

48

52

60

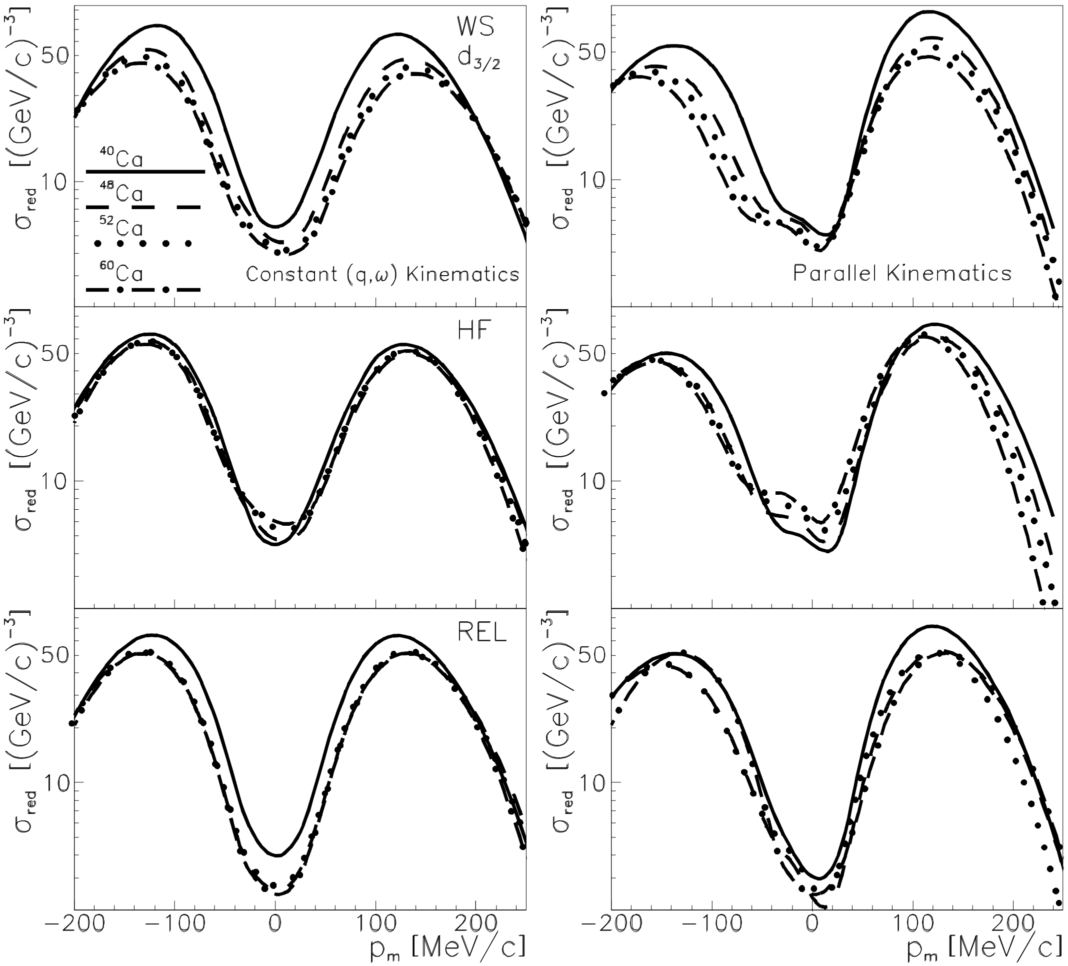

DWIA-WS

DWIA-HF

RDWIA

constant (q,ω)

parallel

C.Giusti et al. PRC 024615 (2011)

$^{40,48,52,60}Ca(e,e'p)$

$d_{3/2}$

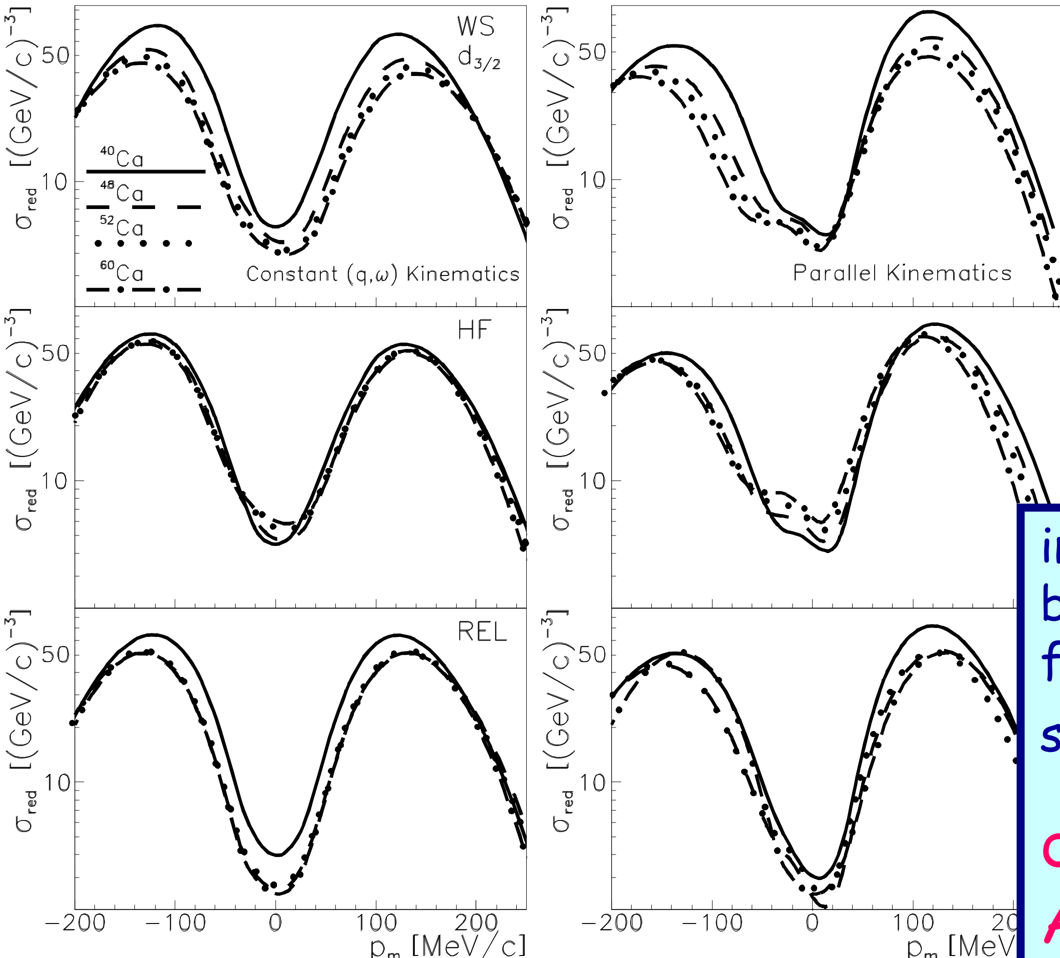

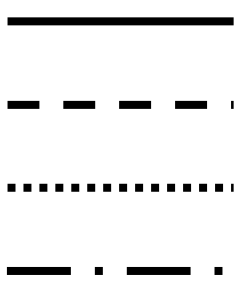

DWIA-WS

DWIA-HF

increasing N/Z different behavior for the wave functions and the cross sections: FSI

difference due to the A- dependence of the optical potential

constant (q,ω)

parallel

C.Giusti et al. PRC 024615 (2011)

- (e,e′p) measurements offer a unique opportunity for studying the dependence of the properties of bound protons on N/Z
- DWIA-WS DWIA-HF RDWIA: good and similar description of the available (e,e′p) data on ^{40}Ca and ^{48}Ca
- DWIA-WS DWIA-HF RDWIA: analogous behavior increasing N/Z asymmetry:
- the different s.p. bound-state w.f. responsible for only a part of the differences, an important contribution is given also by FSI described in the calculations by phenomenological optical potentials
- OP affects the size and the shape of the cross section in a way that strongly depends on kinematics: its dependence on N/Z deserves careful investigation

- (e,e′p) measurements offer a unique opportunity for studying the dependence of the properties of bound protons on N/Z
- DWIA-WS DWIA-HF RDWIA: good and similar description of the available (e,e′p) data on ^{40}Ca and ^{48}Ca
- DWIA-WS DWIA-HF RDWIA: analogous behavior increasing N/Z asymmetry:
- the different s.p. bound-state w.f. responsible for only a part of the differences, an important contribution is given also by FSI described in the calculations by phenomenological optical potentials
- OP affects the size and the shape of the cross section in a way that strongly depends on kinematics: its dependence on N/Z deserves careful investigation

$\Downarrow$

OPTICAL POTENTIAL

OPTICAL POTENTIAL

- (e,e′p): in DWIA bound and scattering states are eigenfunctions of a non-Hermitian energy-dependent OP and should be obtained from a consistent microscopic many-body calculation
- (e,e′p): in DWIA calculations phenomenological OPs are usually adopted
- OP describes elastic nucleon-nucleus scattering
- phenomenological and theoretical OP

OPTICAL POTENTIAL

PHENOMENOLOGICAL: assume a form and a dependence on a number of adjustable parameters for the real and imaginary parts that characterize the shape of the nuclear density distribution and that vary with the nuclear energy and the nucleus mass number.

Parameters obtained through a fit to pA elastic scattering data

THEORETICAL: microscopic calculations require the solution of the full many-body nuclear problem. Some approximations are needed.

We do not expect better description of experimental data but greater predictive power when applied to situations where exp. data not available

M. Vorabbi, P. Finelli, C. Giusti, PRC 93 034619 (2016)
Theoretical optical potential derived from nucleon-nucleon chiral potentials

M. Vorabbi, P. Finelli, C. Giusti, PRC 93 034619 (2017)
Theoretical optical potential derived from nucleon-nucleon chiral potentials at **N^4LO**

Purpose: study the domain of applicability of microscopic two-body chiral potentials to the construction of an OP

Theoretical framework for pA elastic scattering

We start from the full (A+1) body LS equation

$$T = T + VG_0(E)VT$$

Separation into two coupled integral equations

$$T = U + G_0(E)PT$$

$$U = V + VG_0(E)QU$$

T transition op. for elastic scattering,

U OP

Free propagator	Projection operators	Free Hamiltonian	External interaction
$G_0(E)=(E-H_0+i\epsilon)^{-1}$	$P+Q=1$	$H_0=h_0+H_A$	$V=\sum_{i=1}^{A} v_{0i}$

The spectator expansion

Consistent framework to calculate U and T

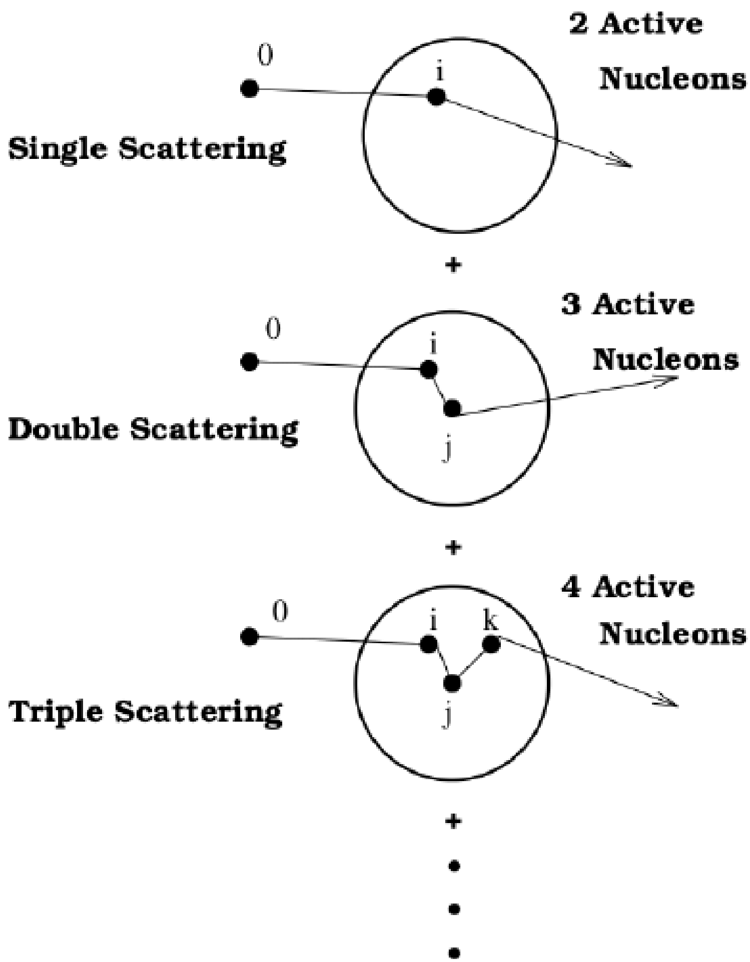

$$
\begin{aligned}
U &= \sum_{i=1}^{A} \tau_i \\
&+ \sum_{i,j\neq i}^{A} \tau_{ij} \\
&+ \sum_{i,j\neq i,k\neq i,j}^{A} \tau_{ijk} \\
&+ \cdots
\end{aligned}
$$

The spectator expansion

Consistent framework to calculate U and T

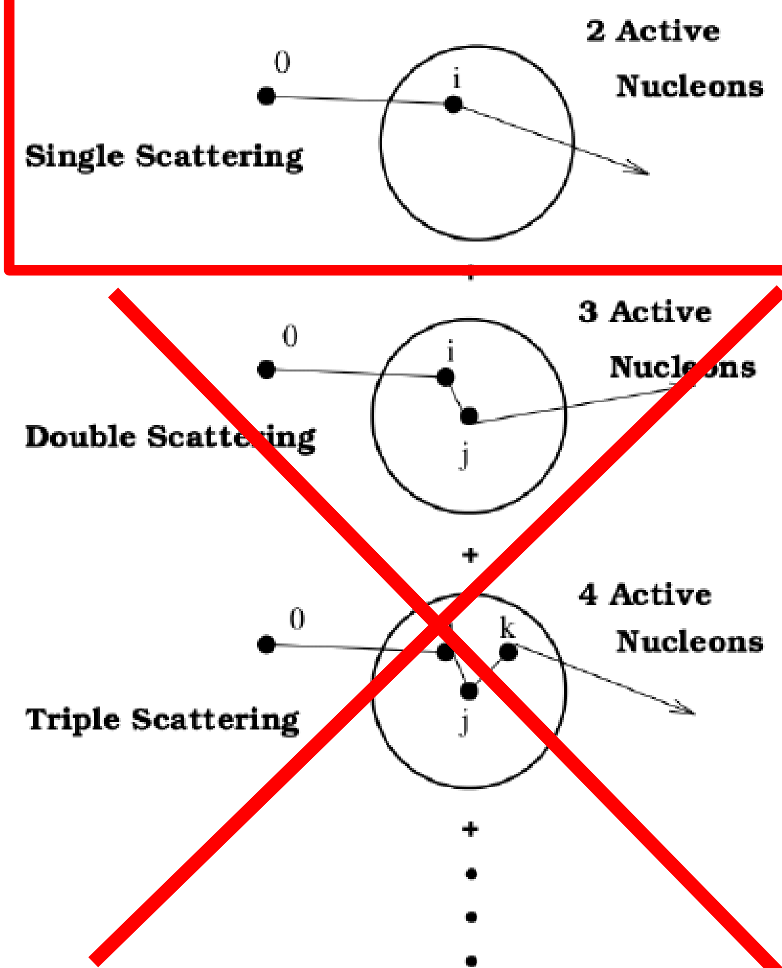

$$U = \sum_{i=1}^{A} \tau_i \; \cancel{+ \sum_{i,j\neq i}^{A} \tau_{ij} + \sum_{i,j\neq i,k\neq i,j}^{A} \tau_{ijk} + \cdots}$$

Impulse Approximation

$$\tau_i \approx t_{0i}$$

The free NN t matrix

$$t_{0i} = v_{0i} + v_{0i} g_i t_{0i}$$

The free two-body propagator

$$g_i = \frac{1}{E - h_0 - h_i + i\epsilon}$$

$$\boxed{U = \sum_{i=1}^{A} t_{0i}}$$

Impulse Approximation

$$\tau_i \approx t_{0i}$$

The free NN t matrix

$$t_{0i} = v_{0i} + v_{0i} g_i t_{0i}$$

The free two-body propagator

$$g_i = \frac{1}{E - h_0 - h_i + i\epsilon}$$

$$\boxed{U = \sum_{i=1}^{A} t_{0i}}$$

We have to solve only 2-body equations

Optimum Factorization Approximation

$$U(\boldsymbol{q}, \boldsymbol{K}; \omega) = \frac{A-1}{A}\, \eta(\boldsymbol{q}, \boldsymbol{K}) \sum_{N=n,p} t_{pN}\left[\boldsymbol{q}, \frac{A+1}{A}\boldsymbol{K}; \omega\right] \rho_N(q)$$

NN t-matrix
NN interaction

n, p densities

$\boldsymbol{q} = \boldsymbol{k}' - \boldsymbol{k}$ $\boldsymbol{K} = \frac{1}{2}(\boldsymbol{k}' + \boldsymbol{k})$

Optimum Factorization Approximation

$$U(\boldsymbol{q},\boldsymbol{K};\omega)=\frac{A-1}{A}\,\eta(\boldsymbol{q},\boldsymbol{K})\sum_{N=n,p} t_{pN}\left[\boldsymbol{q},\frac{A+1}{A}\boldsymbol{K};\omega\right]\;\rho_N(\boldsymbol{q})$$

NN t-matrix
NN interaction

n, p densities

$$\boldsymbol{q}=\boldsymbol{k}'-\boldsymbol{k} \qquad\qquad \boldsymbol{K}=\tfrac{1}{2}(\boldsymbol{k}'+\boldsymbol{k})$$

- n,p densities calculated within the RMF description of spherical nuclei using a DDME model
- NN interaction chiral potentials…

CHIRAL POTENTIAL

- When the concept of EFT was applied to low-energy QCD, ChPT was developed
- Within ChPT it became possible to implement chiral symmetry consistently in a theory of pionic and nuclear interactions
- The theory is based on a perturbative expansion in powers of $(Q/\Lambda_\chi)^n$ where Q is the magnitude of the three-momentum of the external particles or the pion mass and Λ_χ is the chiral symmetry breaking scale of the chiral EFT
- From the perturbative expansion only a finite number of terms contribute at a given order

CHIRAL POTENTIAL

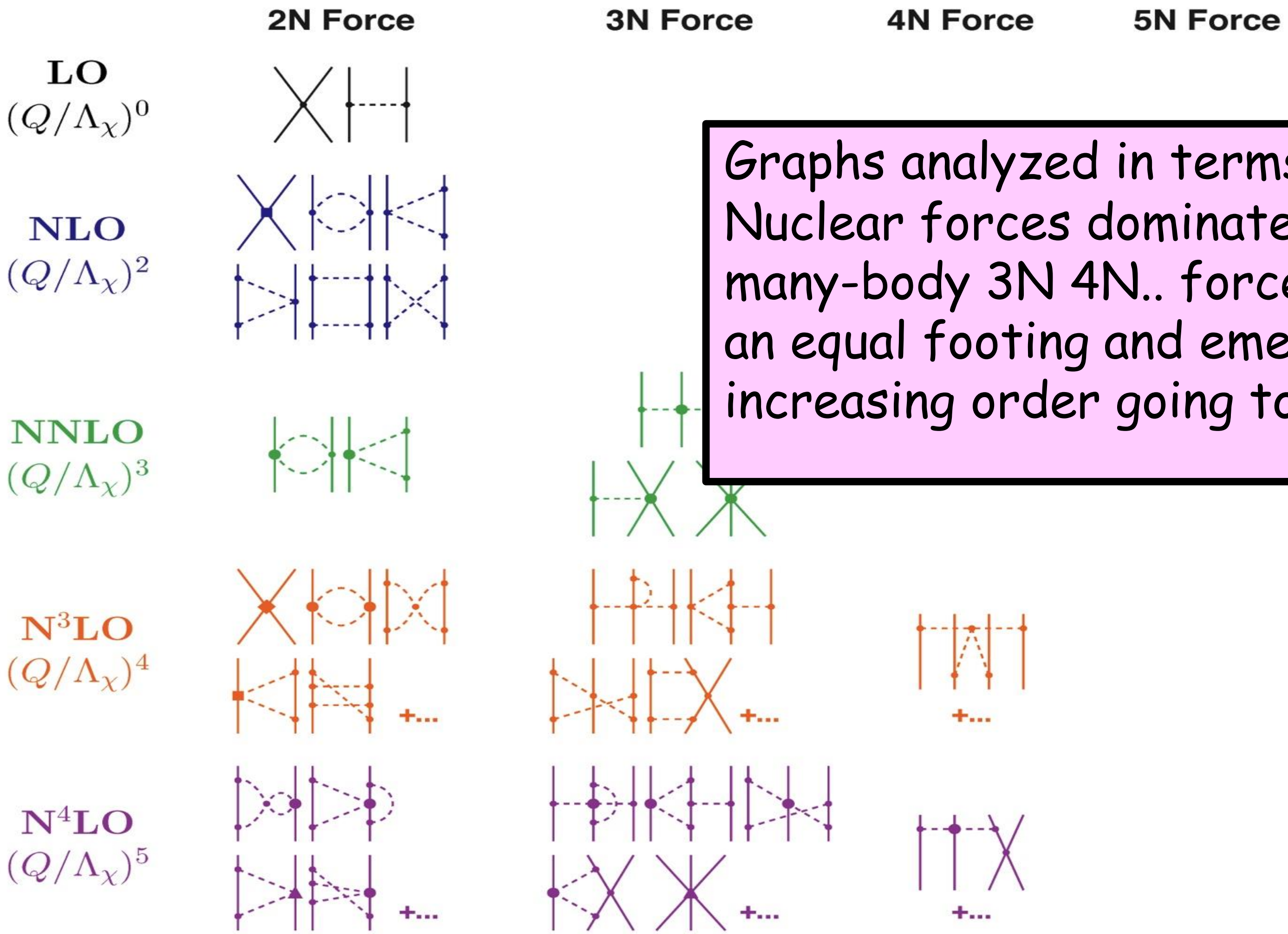

Graphs analyzed in terms of $(Q/\Lambda_\chi)^n$
Nuclear forces dominated by NN int.
many-body 3N 4N.. forces created on an equal footing and emerge in increasing order going to higher order

CHIRAL POTENTIAL

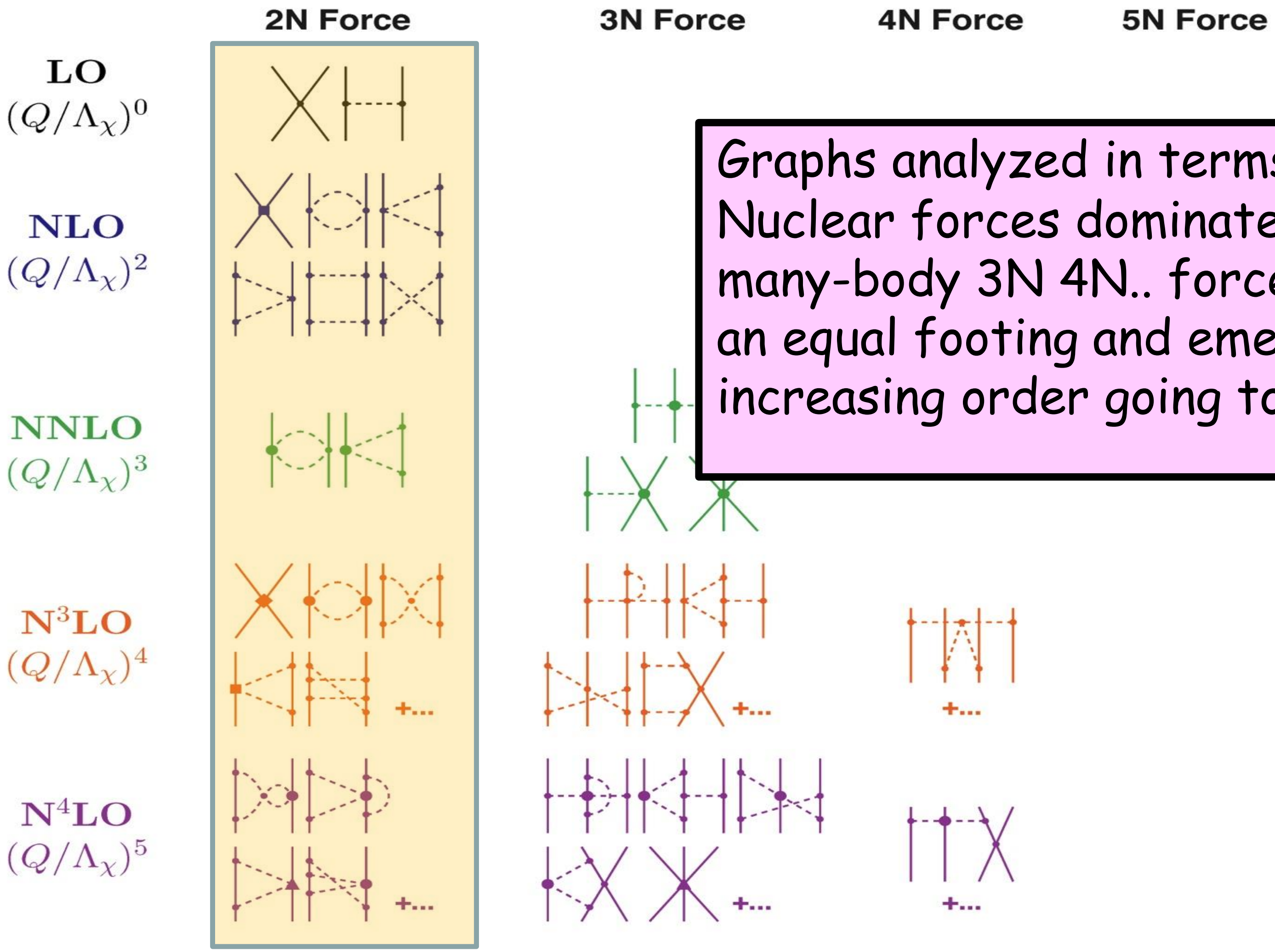

Graphs analyzed in terms of $(Q/\Lambda_\chi)^n$
Nuclear forces dominated by NN int.
many-body 3N 4N.. forces created on an equal footing and emerge in increasing order going to higher order

E. Epelbaum et al. . PRL 115 122391 (2015), EPJA 51 53 (2015) EKM

D.R. Entem et al. PRC 91 014002 (2015), PRC 96 024004 (2017) EMN

M. Vorabbi, P. Finelli, C. Giusti, PRC 93 034619 (2016)

Theoretical optical potential derived from nucleon-nucleon chiral potentials

order by order convergence: it is mandatory to use chiral potentials at N^3LO to describe elastic pA and NN scattering data

M. Vorabbi, P. Finelli, C. Giusti, PRC 93 034619 (2017)

Theoretical optical potential derived from nucleon-nucleon chiral potentials at N^4LO

Purpose: check the convergence and assess the theoretical errors associated with the truncation of the chiral expansion in the construction of an OP

M. Vorabbi, P. Finelli, C. Giusti, PRC 93 034619 (2017)

Theoretical optical potential derived from nucleon-nucleon chiral potentials at N^4LO

Purpose: check the convergence and assess the theoretical errors associated with the truncation of the chiral expansion in the construction of an OP

Results: robust convergence has been reached at N^4LO, agreement with data neither better nor worse than with chiral NN potentials at N^3LO

^{16}O **200 MeV** ^{40}Ca

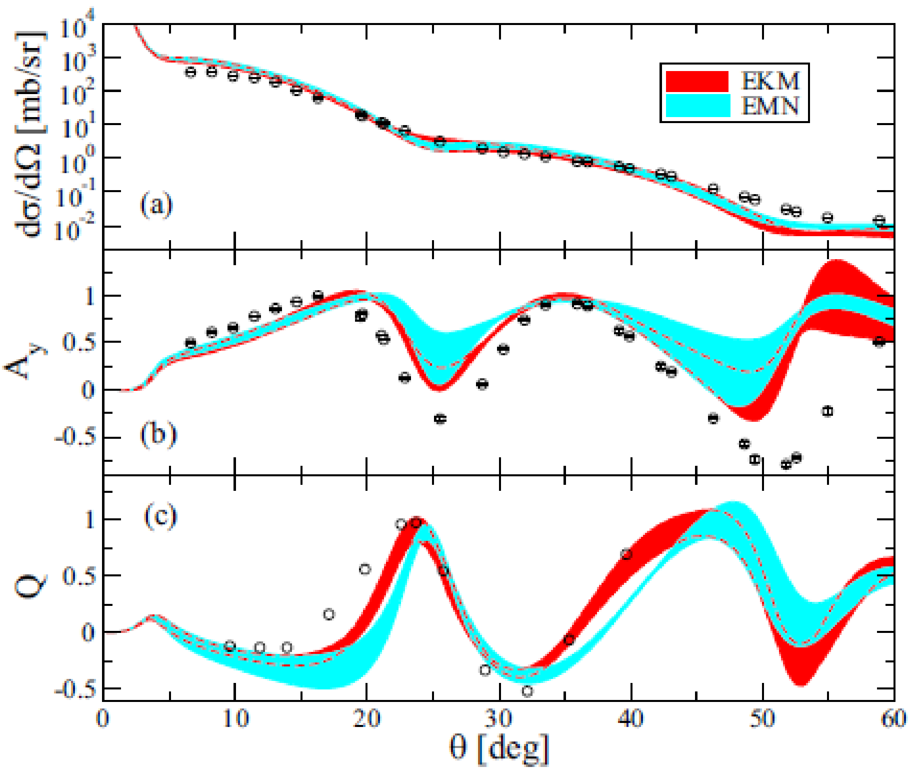

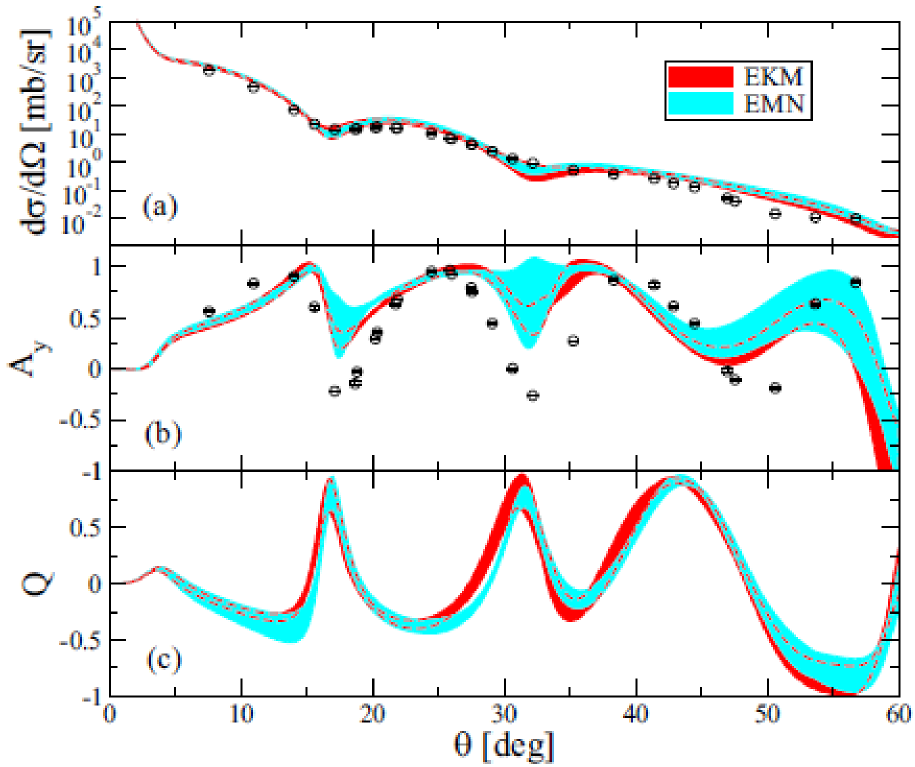

M. Vorabbi, P. Finelli, C. Giusti PRC 96 044001 (2017)

Comparison with phenomenological OP

- investigate and compare predictive power of our microscopic OP and of phenomenological OP in comparison with exp. data in a wider range of nuclei, including isotopic chains

M. Vorabbi, P. Finelli, C. Giusti, arXiv:1806.01037v1 (2018)
Proton-Nucleus Elastic Scattering: Comparison between Phenomenological and Microscopic Optical Potentials

Comparison phenomenological and microscopic OP

PHENONOMENOLOGICAL OP

GLOBAL given in a wide range of nuclei and energies

NROP up to ~200 MeV, for higher energies it is generally believed that the Schroedinger picture should be taken over by a Dirac approach. Global ROP available up to ~1 GeV

NROP Koning at al. NPA 713 231 (2003) (KD) for nuclei $24 \leqslant A \leqslant 209$ and energies from 1 keV to 200 MeV, more recently extended to 1 GeV, to test at which energy the predictions of a phen. NROP fail

Calculations with TALYS (ECIS-06)

MICROSCOPIC OP
chiral potentials at N^4LO describe NN scattering data up to 300 MeV and our OP can be used up to ~ 300 MeV

Comparison phenomenological and microscopic NROP

PHENONOMENOLOGICAL OP

GLOBAL given in a wide range of nuclei and energies

NROP up to ~200 MeV, for higher energies it is generally believed that the Schroedinger picture should be taken over by a Dirac approach. Global ROP available up to ~1 GeV

NROP Koning at al. NPA 713 231 (2003) (KD) for n
and energies fro
more recently ex
test at which ene
of a phen. NROP fail

Calculations with TALYS (ECIS-06)

MICROSCOPIC OP
chiral potentials at N^4LO describe NN scattering data up to 300 MeV and our OP can be used up to ~ 300 MeV

Results of the comparison in the energy range 150-330 MeV

Comparison with phenomenological OP

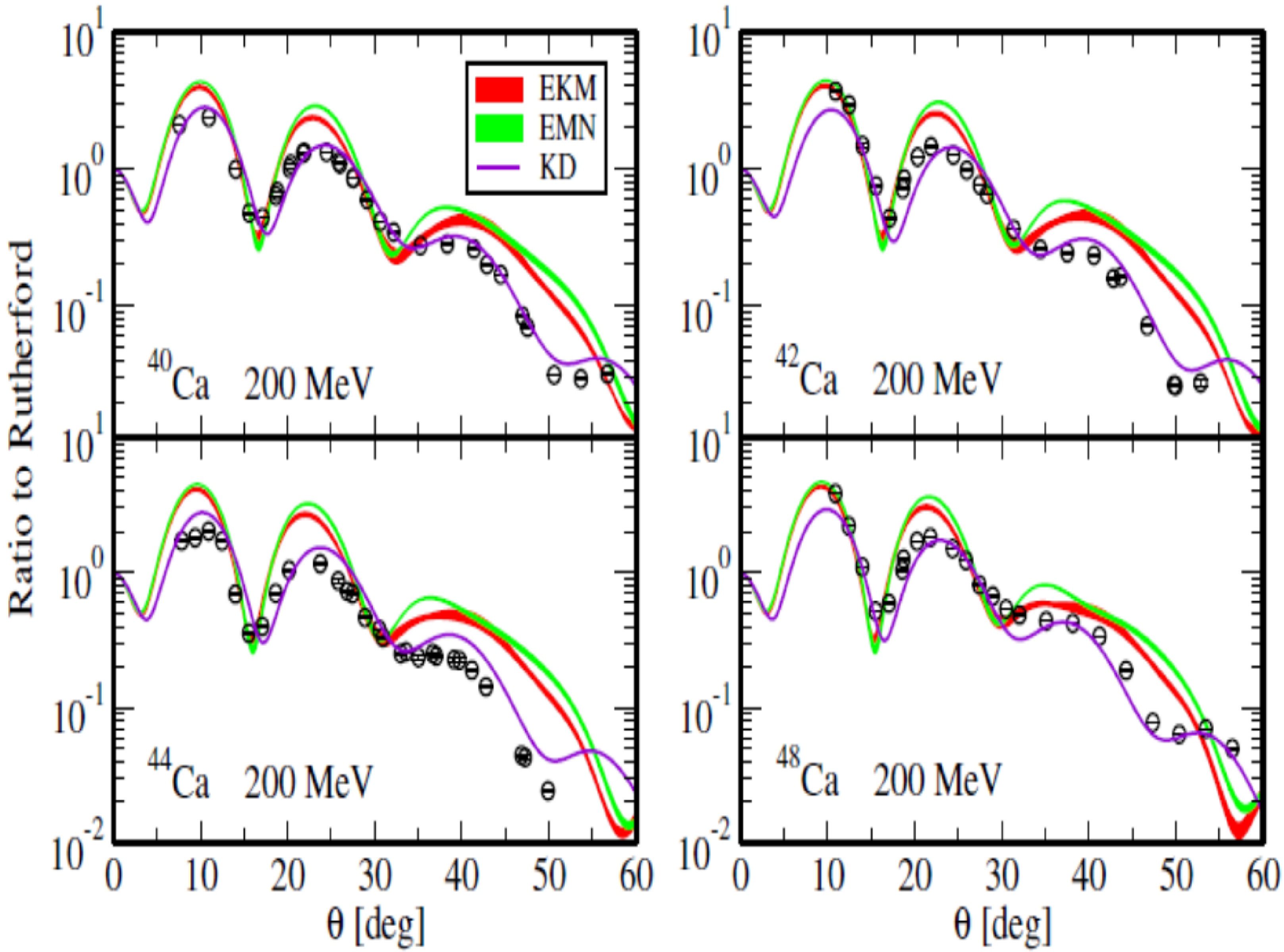

Comparison with phenomenological OP

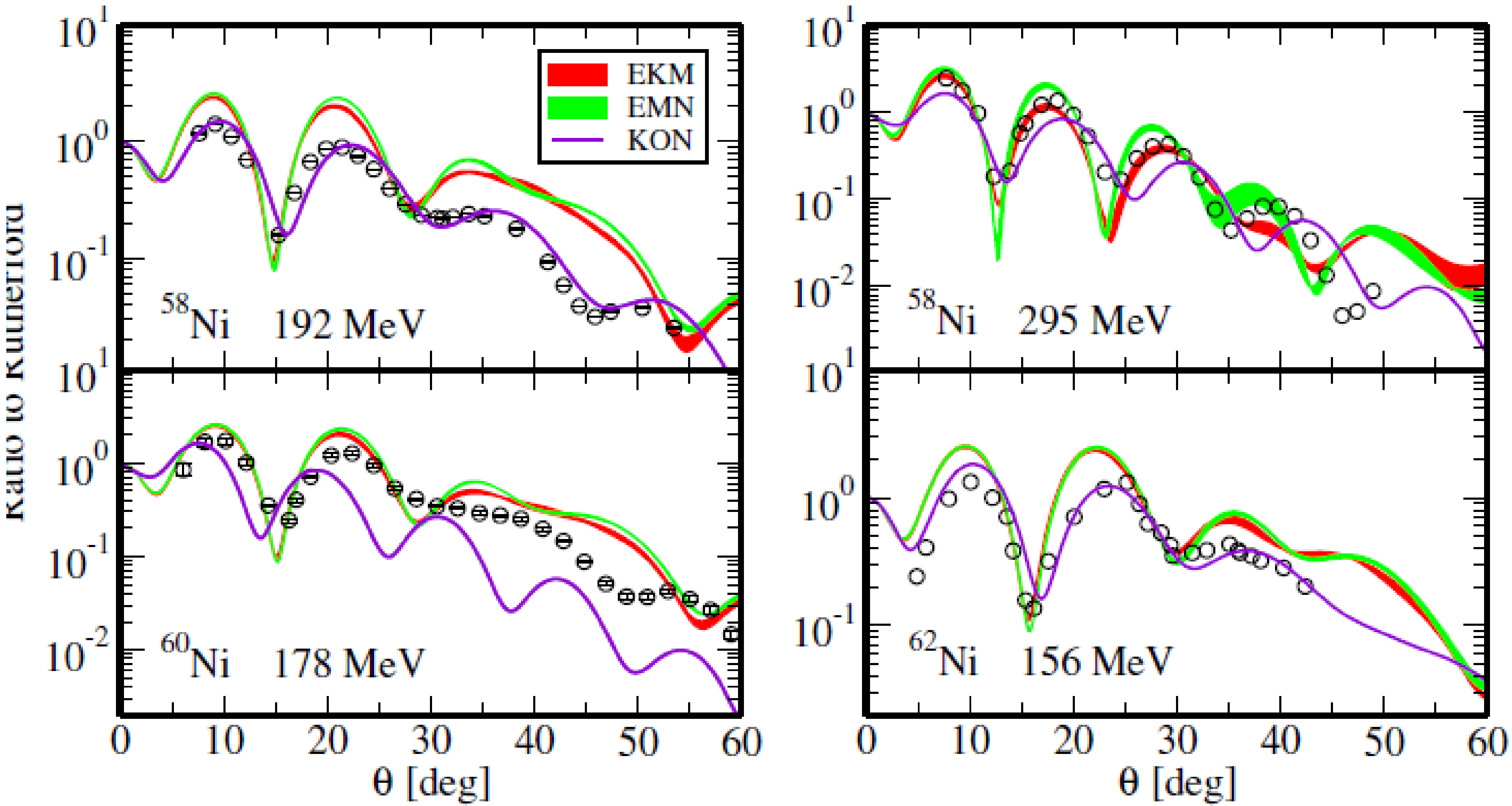

Comparison with phenomenological OP

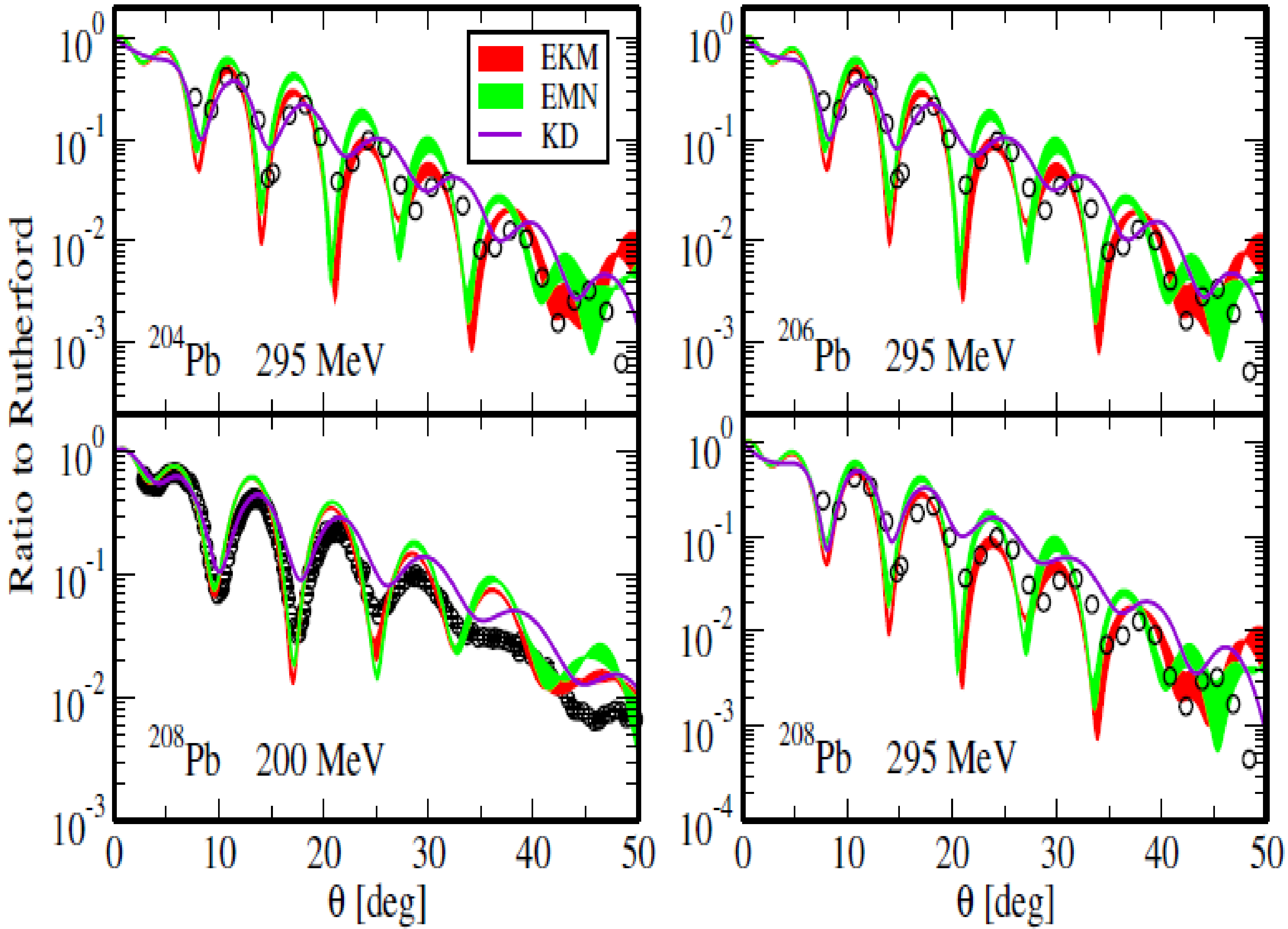

Comparison with phenomenological OP

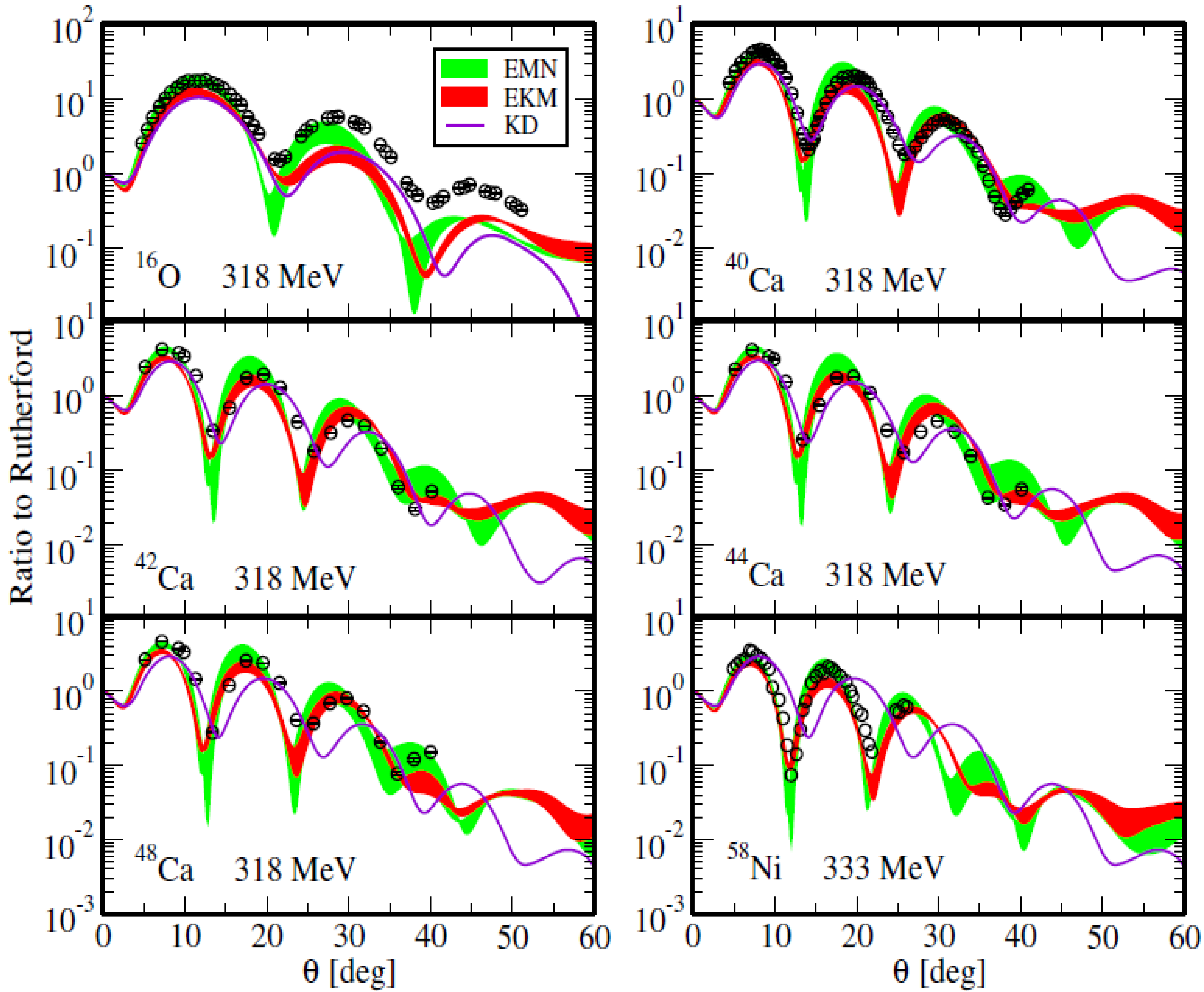

PROSPECTS...

- the model can be improved
- folding integral
- 3N forces, medium effects
- application to nuclear reactions.... (e,e'p)